

For: Dr. Fred. K. Duennebier

Fu

**IN SITU ACOUSTIC PROFILES OF THE
SEDIMENT-SEAWATER INTERFACE**

A THESIS SUBMITTED TO THE GRADUATE DIVISION OF THE
UNIVERSITY OF HAWAII IN PARTIAL FULFILLMENT OF THE
REQUIREMENT FOR THE DEGREE OF

MASTER OF SCIENCE

IN GEOLOGY AND GEOPHYSICS

SEPTEMBER 1994

By

Shung-sheng Fu

THESIS COMMITTEE:

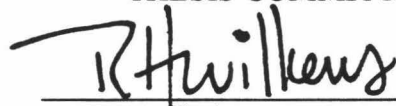
Roy H. Wilkens, Chairperson

L. Neil Frazer


Fred K. Duennebier

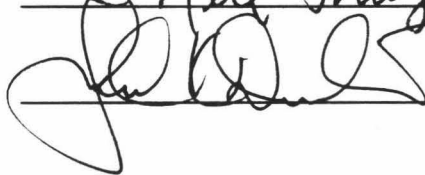
We certify that we have read this thesis and that, in our opinion,
it is satisfactory in scope and quality as a thesis for the degree of Master of
Science in Geology and Geophysics.

THESIS COMMITTEE



Chairperson





Dedication

This thesis is dedicated to my mother,

and in memory of my father.

Acknowledgements

I would like to thank Dr. Roy H. Wilkens most of all for his guidance, support, and patience throughout the all aspects of this research. Thanks are also extended to Dr. L. Neil Frazer and Fred K. Duennebier for their expertise and willingness to be members of the thesis examining committee. Dr. L. Neil Frazer and Dr. Authur Cheng of MIT gave their invaluable guidances in signal processing. Thanks go to Lance design engineer James Jolly for his excellent design and Dr. Dae Choul Kim (National Fisheries University of Pusan, S. Korea) for his help and cooperation. The funding for this project was supplied by Office of Naval Research. Thanks also go to my colleagues Jack Kronen and Patrick Jonke for their expertise in laboratory core sample measurements. Jack Kronen also provided me with many suggestions and help in compiling this thesis. A special thanks goes to my family for their encouragement, patience and support.

Abstract

In order to obtain in situ compressional wave velocity and attenuation data to several meters depth in the seafloor, a device, Lance, has been built and deployed in the sediment ponds on the west flank of the Mid-Atlantic Ridge. Lance-the first instrument of its kind, a hybrid of heat-flow piston coring techniques with the principle of a full waveform acoustic logging tool has been proved a useful instrument for increasing our knowledge of the geo-acoustic structure of the sediment-seawater interface.

A comprehensive experiment was carried out in Mid-Atlantic Ridge sediment ponds Lance made in situ measurements, and core samples were recovered. Lance's in situ data were compared with the laboratory data of core samples. These are the first measurements of velocity and attenuation profiles of the upper several meters of the seafloor. Lance data indicate that there is an acoustic channel much thinner than estimated by Hamilton's and Ogushwitz's results.

Table of Contents

Dedication	iii
Acknowledgements	iv
Abstract	v
List of Tables	viii
List of Figures	ix
Introduction	1
Configuration and Working Principle of Lance.....	2
Electronic Principle	4
Control Circuit	4
Analog Circuit.....	6
Digital Circuit	6
Storage Circuit	7
Data Retrieval Interface	7
Firing Circuit.....	8
Power Supply and Power Supply Control.....	8
Acoustic Principle	8
Source.....	8
Receiver	9
Transducer Matching	11
Receiver Mounting.....	13
Acoustic Background	15
Signal Analysis and Data Processing.....	16
Velocity Data	18
Attenuation Data	22
Methods to Estimate Q.....	22
Spectral ratios.....	22
Q-gram	32
Field Application.....	34
General Geological Description of the Field Area.....	34
Field Operation	40
Data Analyses and Results	44
In Situ Velocity Profiles.....	45
Laboratory Velocity Data.....	50
A Hypothesis	57

In Situ Q Profile	61
Discussion and Conclusions.....	64
Instrumentation	64
In Situ Experiment of the Sediment Pond.....	64
References	66

List of Tables

<u>TABLE</u>		<u>PAGE</u>
Table 1.	The Locations of In Situ Measurements and Coring.	41
Table 2.	The Velocity Data of 5 Measurements In Station #6.....	46
Table 3.	The velocity Data of 5 Stations (#1 - #5)	46

List of Figures

<u>FIGURE</u>	<u>PAGE</u>
Figure 1. The Configuration of Lance.	3
Figure 2. Block Diagram of Electronics of Lance.	5
Figure 3. The Power Spectrum of A Signal Received in Water.	10
Figure 4. Recorded Signals from 6 Receivers at Same Position in Water.	12
Figure 5. The Holder for AQ-1 Hydrophone.	14
Figure 6. The Procedure Block Diagram of Signal Processing.	19
Figure 7 The Original Signal and Interpolated Signal.	21
Figure 8. The Waveforms of Signals Received in Shallow water and Deep water.	23
Figure 9. The Travel time error Caused by Distorted Waveform.	24
Figure 10. Determination of Q by Power Spectral Ratio.	27
Figure 11. Selection of the Truncation Window.	29
Figure 12. Comparison of Spectral Ratio With and Without Velocity Dispersion.	30
Figure 13. Bathymetry of the Sediment Pond.	35
Figure 14. Bathymetry Chart of Site A and Site D.	36
Figure 15. Bathymetry Chart of Site B' and Site C'.	37
Figure 16. A photomicrograph of Core #1 Sample.	38
Figure 17. A photomicrograph of Core #5 Sample.	39
Figure 18. The Waveforms of Received Signals from 5 Stations (#1 - #5).	42
Figure 19. Waveforms from One Deployment at Station #6.	43
Figure 20. Velocity Profiles at Station #6.	47
Figure 21. Velocity Profiles of 5 Stations (#1 - #5).	48
Figure 22. Comparison of In Situ Data and Laboratory Data of Velocity in Site B'.	51
Figure 23. The Procedure Block Diagram for Analysis of In Situ Data and Laboratory Data.	52
Figure 24. Velocity and Porosity Distributions of Core #1 - #3.	55

Figure 25. Velocity vs Porosity of Cores Measured in Laboratory. 56

Figure 26. Two Plausible Models of Porosity Distribution. 58

Figure 27. Comparison of In Situ Data and Laboratory Data of Velocity in Site
A..... 59

Figure 28. Layered Sediment Model..... 60

Figure 29. The Procedure Block Diagram for Rough Q Estimation. 62

Figure 30. The Estimation of Q by Synthetic Propagation. 63

Introduction

The acoustic behavior of the bottom-water interface is of considerable interest in underwater acoustics and geophysics. A large number of physical parameters are involved in the acoustic behavior of marine sediments (Ogushwitz, 1985). Acoustic wave velocity and acoustic wave attenuation are the two most important geoacoustic parameters that directly govern the effects of acoustic and seismic processes at the seafloor. In all shallow-water environments, and in many deep-water cases as well, the seabed is the dominant factor controlling wave propagation. A lossy seabed; where acoustic waves are attenuated within the sediments, causes attenuation of the waterborne sound through both compressional-wave (P wave) absorption in the bottom and the excitation of shear (S) waves (Kibblewhite, 1989). Acoustic velocity and attenuation help to provide a better understanding of the physical properties of marine sediments.

Compressional velocity and attenuation of marine sediments can be estimated using empirical relationships of Hamilton (1971; 1976; 1987), or they can be calculated from physical models such as the Biot-Stoll Model (Ogushwitz, 1985). Direct measurements of velocity and attenuation can be carried out in the laboratory or in situ (field). The in situ data appear to be more reliable than the laboratory data. In situ measurements include the combined effects of the surrounding environment. Accurate laboratory measurements of compressional waves attenuation are restricted to frequencies of 10-20 kHz and above, because the sample dimensions must be much larger than the wavelength of the propagating wave. In the past, extensive measurement programs were conducted and advanced instruments were designed in order to measure the velocity and attenuation in the laboratory. In this thesis, we describe a more accurate

and convenient technique for in situ measurement enabling a change of from laboratory measurement to in situ recording.

The acoustic 'Lance' is an instrument that has been developed to obtain in situ compressional wave velocity and attenuation (Q^{-1}) profiles for a sedimentary layer of several meters thickness at the sediment-seawater interface. Lance is a fullwave and self-contained system consisting of a wide-band source, ten independent receiving channels, and a data storage system. The whole device may attach to a gravity corer or piston corer with 10 receivers arrayed on the corer pipe at known intervals. The received signals are stored in the memories of each channel. Velocity, attenuation and other useful information are subsequently extracted from the received signal by using signal processing techniques. Core samples can be recovered at the same time. As all information obtained depends only on the differences between the signal recorded by different receivers but not only the signal itself, source function changes with environments, such as pressure and temperature, are self-cancelling.

Configuration and Working Principle of Lance

The Acoustic Lance can be broken down into two parts. One is mechanical and the other is electronic and acoustic. Figure 1 illustrates the configuration of Lance. The mechanical part may be a gravity corer, a piston corer, or a specially designed probe. The electronic system includes a receiving circuit, a firing circuit, and a power supply contained in two pressure vessels.

The source transducer and two pressure vessels are installed at the top of the corer. Ten receivers correspond to 10 independent receiving channels that are arrayed on the corer pipe, each with a known interval. The greatest working depth of Lance is about 7000 meters (about 10000 psi).

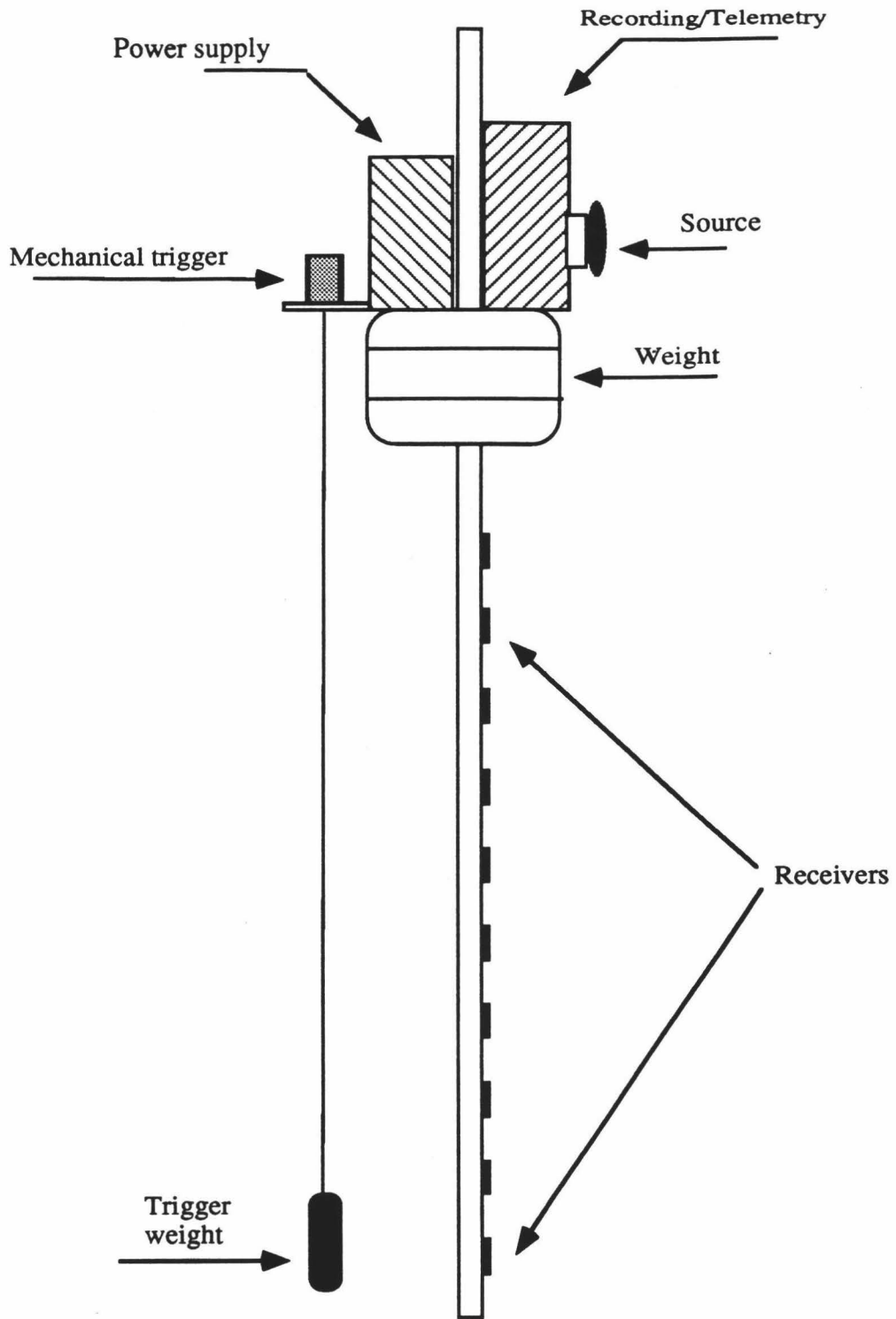


Figure 1. The Configuration of Lance

A mechanical trigger switches Lance from a sleeping state to a working state when the corer touches the seafloor. The trigger will also turn off an acoustic transmitter (high power pinger) when Lance is used in a deep water environment. After a short delay time (15 seconds or two minutes), the source emits a ping. The propagated sound wave is vertically incident upon the seafloor. The corer pipe that has penetrated into the sediments has regularly spaced receivers to collect signals that propagated through the sediments. All received signals are stored in their respective channel memories. The collected data are transferred to the computer after Lance returns to the ship.

Electronic Principle

The receiving system of Lance consists of a control circuit with 10 independent receiving channels. Each channel has an analog circuit, a digital circuit and a storage circuit. Figure 2 is the circuit block diagram. The control circuit accepts preset parameters from the computer program and controls the transfer of data into the computer. These parameters include number of pings, number of samples, and the gain for each channel. The received signals from each channel are amplified, passed through an anti-alias 40k low-pass filter, digitized in a 12 bit 100k A/D converter and stored in 64k of available memory. An SCR (silicon control rectifier) pulse generator provides an 800v pulse to the source transducer.

Control Circuit

All circuits in Lance are operated by the control circuit. It accepts the preset parameters and computer commands from the computer program and produces clock signals. Each ping emitted from the source transducer is assigned a specific start address in memory (SRAM) that is monitored by the control circuit. The trigger signal coming from the mechanical trigger is also sent to the control circuit. The computer communicates with this circuit through an RS-232 Serial Common Port. In a typical ship's working environment, 100-200 feet of cable connects Lance on deck to the

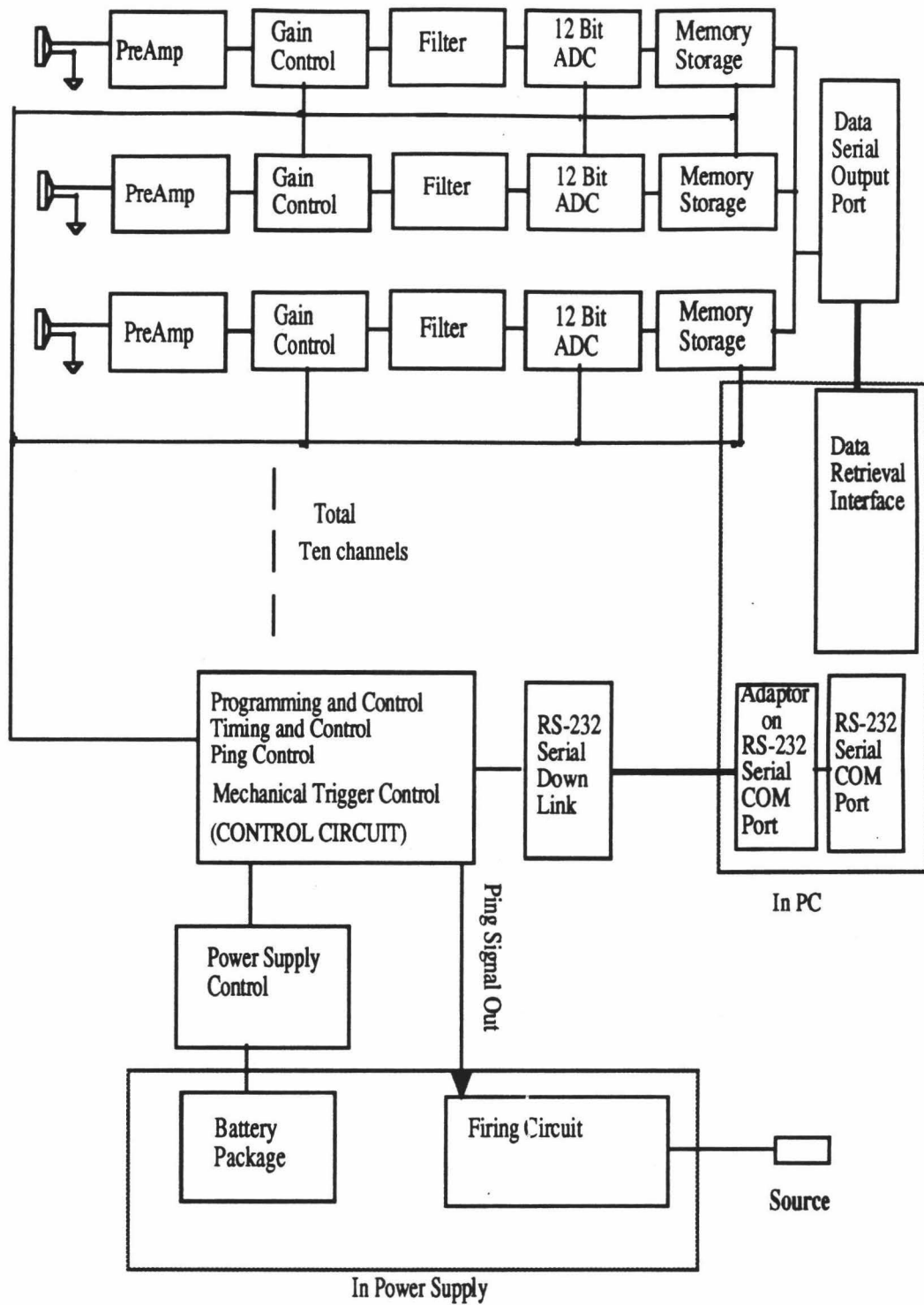


Figure 2. Block Diagram of Electronics of Lance

computer inside the ship's laboratory. Transmitting a short pulse signal by long cable can sometimes cause a timing problem due to the irregular distribution of capacitance or inductance within the cable, or to noise interference. An 8-bit latch used as buffer has been designed in the input part of the circuit in order to prevent any timing problems.

Analog Circuit

The analog circuit of each channel consists of a preamplifier, a gain control amplifier and an anti-alias low-pass filter. A choice of 8 gain settings (gain numbers 0-7) can be preset for the amplifier in each channel separately. The greatest gain is 38 dB and the smallest is 0 db. According to experimental results, gain 3 (18dB) is suitable for muddy sediment with a 5 meter acoustic path. The anti-alias low pass filter has a 40kHz corner frequency and 24dB/octave slope.

Digital Circuit

The digital circuit consists of a 12 bit-100kHz A/D converter and an adder. The received analog signals are digitized in the A/D converter at a 10 μ s sampling interval. The sample length in a ping period is determined by the preset parameter sample number. Possible sample lengths are 512, 1024, 2048, 4096 and 8192, which correspond to sample lengths of a received wavelet of about 5ms, 10ms, 20ms, 40ms and 80ms respectively. The accuracy of measurement depends strongly on the sampling rate of the A/D. It is the function of the adder to stack received signals in order to increase the signal-to-noise ratio. Possible ping number parameters (i.e, 1, 2, 4, 8, 16) represent the number of signals that will be stacked in the adder. For a stacked signal the source sends out several pings (according to the preset ping number) at 1 second time intervals. The received signals from each ping are superimposed in the adder and then averaged after the data are retrieved. As a result of stacking, the signal to noise ratio is reduced.

Storage Circuit

There is a 64k x 16 bit memory (SRAM) for each receiver. The digitized data input (output of A/D converter) uses 12 of 16 bits. The other 4 bits are used to determine a sign extension for signal stacking. Each memory cell (one sample point) occupies 32 bits of memory, including its data value and address. The 64k of memory allows Lance to deploy for multiple- measurements. Lance is capable of deploying at the seafloor until the memory in each channel is full. A multiple-measurement is different from signal stacking, in that no extra memory is used in stacking because the received signals are superimposed in the adder before being stored in memory. For a given lowering, the number of mutiple-measurements is related to the sample length of a received wavelet selected. The longer the sample length is, the fewer multiple-measurements are attainable. For example, if a sample length of 2048 points is selected, it can record up to 8 independent measurements, the largest number of points that the memory can store. If the sample length is 1024 points, Lance can receive a 16 multiple-measurements. There is a backup battery in the circuit to prevent Lance from losing data caused by power supply exhaustion or other accidents.

Data Retrieval Interface

The data retrieval interface comprises a serial output port in Lance and a serial data receiver in the computer. The output port retrieves data from SRAM and sends them to the data receiver in serial format. The computer collects the data, displays the waveform on the monitor, and stores the data. Since communication on deck is by a long electronic cable, a pair of high-speed FSK(frequency shift keying) modems are employed, which encode binary data into two discrete frequencies (mark and space frequencies). The mark (logic high) and space (logic low) frequencies of the FSK modem are 5.37MHz and 2.42MHz respectively.

Firing Circuit

The firing circuit is an SCR pulse generator that accepts the firing pulse signal from the control circuit, amplifies this signal and drives the source transducer to produce the pings. A low power inverter supplies 800 volts DC to the pulse generator. The common point (ground line) of the circuit is isolated from the entire system to hinder potential interference of high voltage with the receiving system.

Power Supply and Power Supply Control

Three sets of 12v rechargeable batteries serve as the power supply for Lance. Two of the sets are for the receiving system and firing circuit, and the third is a backup battery for the SRAM. When Lance is in a sleeping state, most working current is cut off by a power control circuit to save power. A set of 8A/hour (4 batteries x 2A/hour) batteries will work continually for about 12 hours.

Acoustic Principle

The acoustic part of Lance consists of the source transducer, the receivers, and their matching network and mounting structure. A distinct first arrival, wide frequency response, and low acceleration response are the main design aims of the acoustic system.

Source

A standard 2.5" x 5" deep water broad-band cylindrical hydrophone is used as the source transducer. It produces source signals with broad-band frequency characteristics and omni-direction. A cylindrical hydrophone has three basic modes of vibration associated with radial, length and thickness dimensions. The resonance frequency of the thickness mode is higher than others and is not involved in the frequency band of Lance. In general, for a resonant transducer designed as a receiver (hydrophone), it is desirable to achieve a response which is independent (or almost independent) of frequency. Therefore a hydrophone should be operated in a band well below its resonance frequencies. However if we use a hydrophone as a projector, we must consider carefully

whether its resonance frequencies are involved in the frequency band we are interested in and the effect of the coupling between the basic modes of vibration. When the hydrophone we use as source is excited by a single pulse there are two basic modes of vibration, the radial mode and the length mode, involved in the frequency band of Lance. The length mode has a resonant frequency of about 16 kHz, and the radial mode 28 kHz. If the source is in a vertical position the received signals should have a center frequency of about 16 kHz, and in horizontal position 28 kHz. However two peaks, about 8 kHz and 16 kHz, appear in the power spectrum of received signals when the source transducer is in vertical position (Fig. 3). A possible reason for this phenomenon is the effect of coupling between the radial mode and the length mode. In theory, a broad source band should facilitate extraction of sediment Q from the signals. We are working to find a more broad band source transducer for the future.

Receiver

We selected AQ-1 cylindrical hydrophones as receivers. Small volume, deep water operation, proper frequency range, wide frequency band and relatively low cost are the main requirements of Lance receivers. The main parameters of the AQ-1 hydrophone are as follows:

Acoustic Sensitivity (dBV re 1 μ Pa, \pm 1 dB)	-202.5 dB
Frequency Response (\pm 1.5 dB)	1 Hz - 10 kHz
Depth -- meter (rated/destruct)	1732/13868
Size -- cm (dia./length)	1.59/4.45
Weight --grams (air/water)	17.3/8.5
Capacity --pfd (\pm 25%)	14, 500

For Lance, a wide frequency receiver band is not only a main requirement for attenuation measurement but also for velocity measurement. A receiver with a wider frequency band (low Q_m factor) has a shorter transient response. It is necessary for

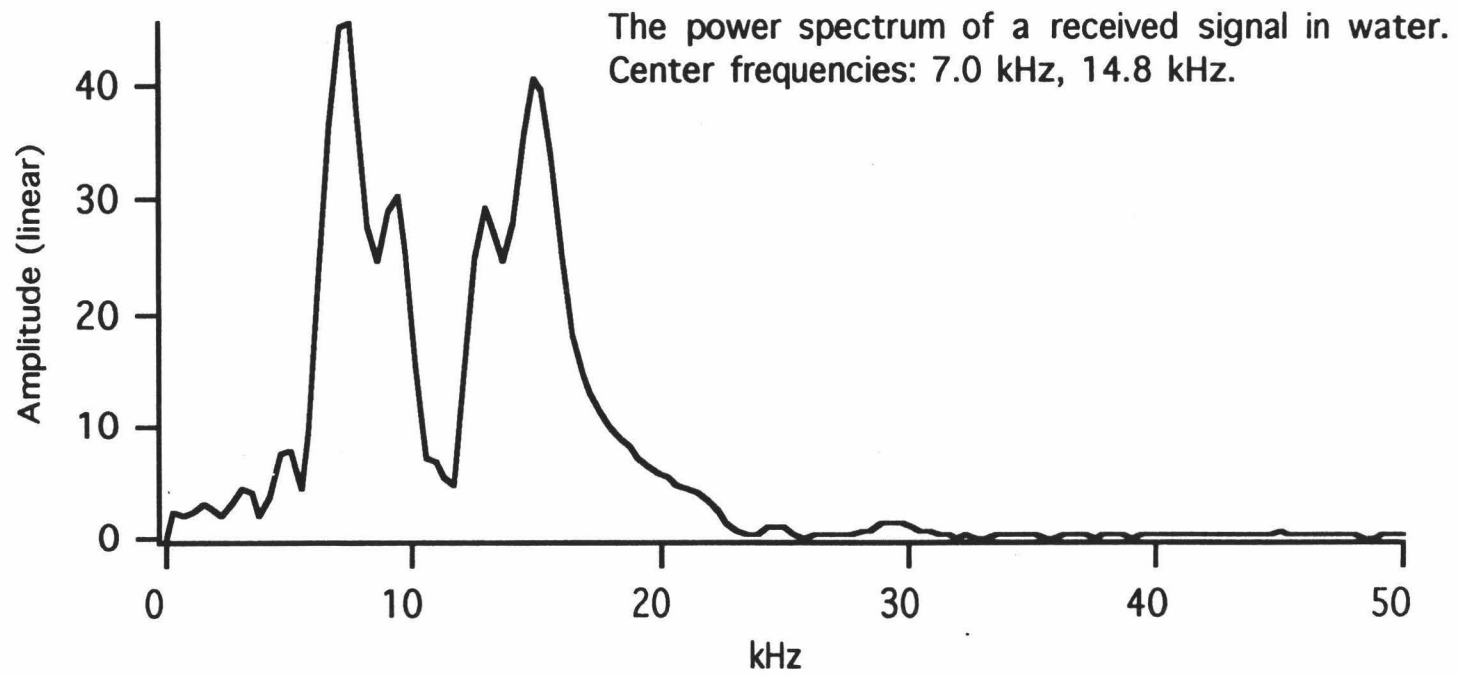


Figure 3. The power spectrum of a signal received in water.

velocity measurements to have a shorter response time because it provides a more distinct first arrival.

The resonant frequency of the source transducer is greater than the flat frequency response (1 Hz-10 kHz) region of the receiver listed above. This is acceptable, because hydrophones always work in regions well below resonant frequency. We estimated the resonant frequency of the radial mode and the length mode of the AQ-1 hydrophone from the dimensions (Stansfield, 1990):

radial mode $f_{rr} = 930 \text{ Hz.m} / 2a = 58 \text{ kHz}$ (a is radius)

length mode $f_{rl} = 1430 \text{ Hz.m} / L = 32 \text{ kHz}$

If the frequency band of 1 kHz- 20 kHz is the region of interest, this band is acceptably below the resonant frequency.

Lance has ten independent channels with ten receivers. It is difficult to make ten receivers with consistent frequency response and sensitivity, especially in the frequency band above the manufacturer's specification. Figure 4 shows the signals in water from six receivers. No two receivers have exactly the same response. Therefore the calibration of the frequency response and sensitivity of every receiver is very important in the calculation of attenuation. We will continue this discussion in the section on Lance signal processing.

Transducer Matching

The source transducer of Lance, which is excited by a single pulse, is connected to a fixed tuning coil in series to promote energy conversion around the resonant frequency and avoid the shorting effect of the pulse generator. As mentioned above, AQ-1 receivers have a flat frequency response in the frequency range from 1 kHz to 20 kHz. A tuning coil is connected in parallel to every receiver to constrain the frequency response to the range 1 kHz to 20 kHz (like a filter) and to improve the waveforms of received signals. When the motional Q-factor of the hydrophone, however, is not low enough, the response

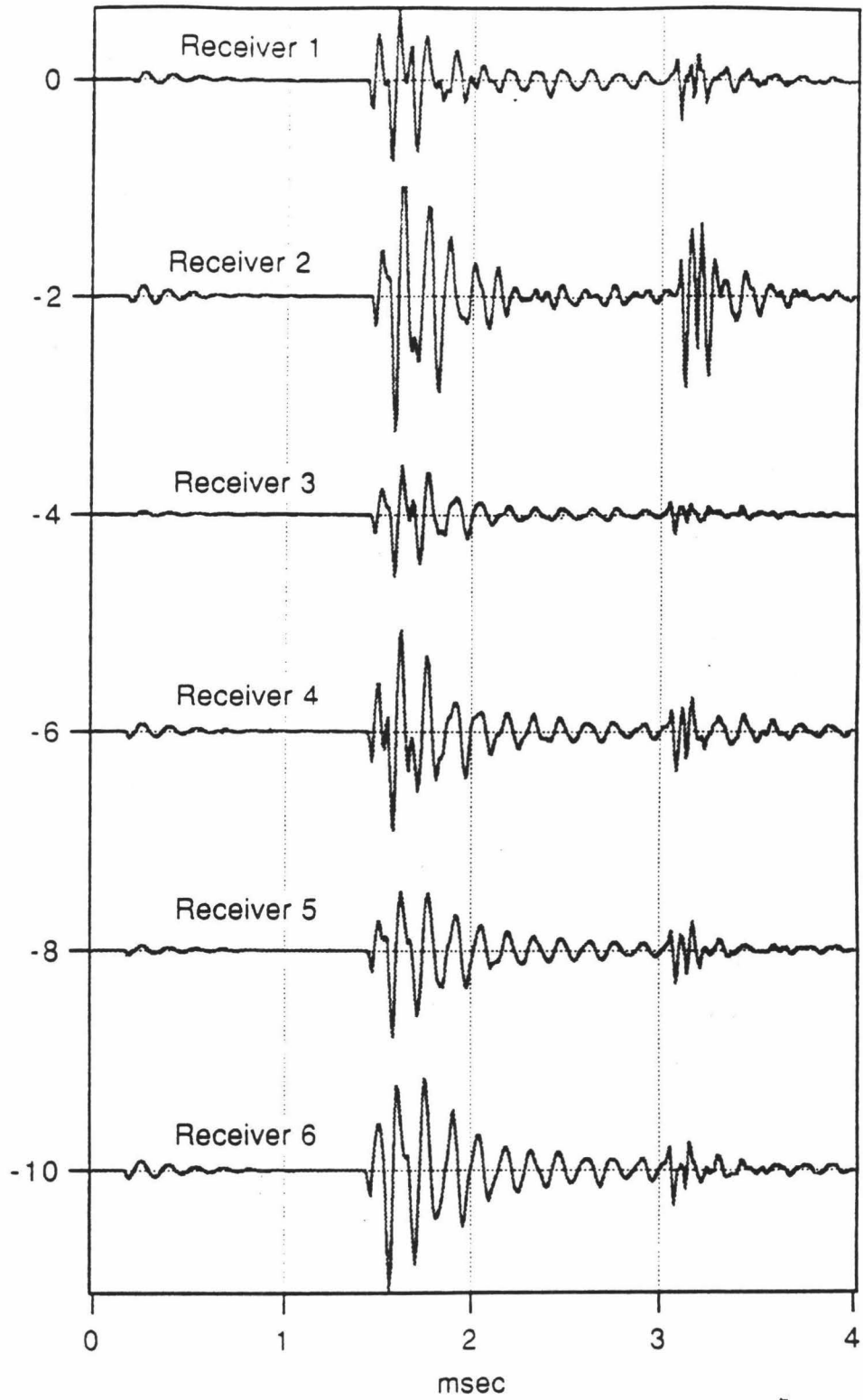


Figure 4. Recorded signals from 6 receivers at same position in water. Receiver transfer functions are clearly different.

curve of a tuned transducer will have two peaks (Stansfield, 1990). This is another possible reason for two peaks in the signal spectra.

Receiver Mounting

The piezoelectric element of any transducer is sensitive to all stresses in the ceramic regardless of how they are caused. Any vibration of the hydrophone mounting produces a stress in the ceramic, accelerating the end-masses in sympathy with supporting structure vibration. The noise due to vibration of mounting is often called the acceleration response of the hydrophone (Stansfield, 1990). If the receivers of Lance are mounted rigidly and directly on the corer pipe or barrel, the vibrations of pipe and the source signals propagating along the pipe will produce high acceleration response in every receiver. The amplitude of the acceleration response might disguise that of the signals propagating in the sediments. On the other hand, the receivers of Lance have to firmly be mounted on the corer pipe to maintain a fixed position, and a structure is needed to protect receivers from the impact when the corer pipe penetrates the seafloor.

The mounting structure of Lance receivers is illustrated in Figure 5. The aim of the mounting structure is to reduce the acceleration response and preserve the receivers. A slice of vulcanized rubber is intercalated between a plastic holder and the wall of the corer pipe to isolate the receiver. There is a standoff with multiple-layers of rubber-aluminium isolating vibration from the corer pipe to the receiver. Two plastic rings filled with epoxy resins form the two ends of the AQ-1 hydrophone. These two plastic rings support the AQ-1 hydrophone in the slot of the holder. The acoustic impedance of the plastic ring is quite different from the PZT ceramic of the AQ-1 hydrophone. It decouples hydrophone from holder. The whole mounting structure keeps the receiver attached rigidly to the corer pipe, but greatly reduces the acceleration response. The mounting structures were tested in air and the result was satisfactory.

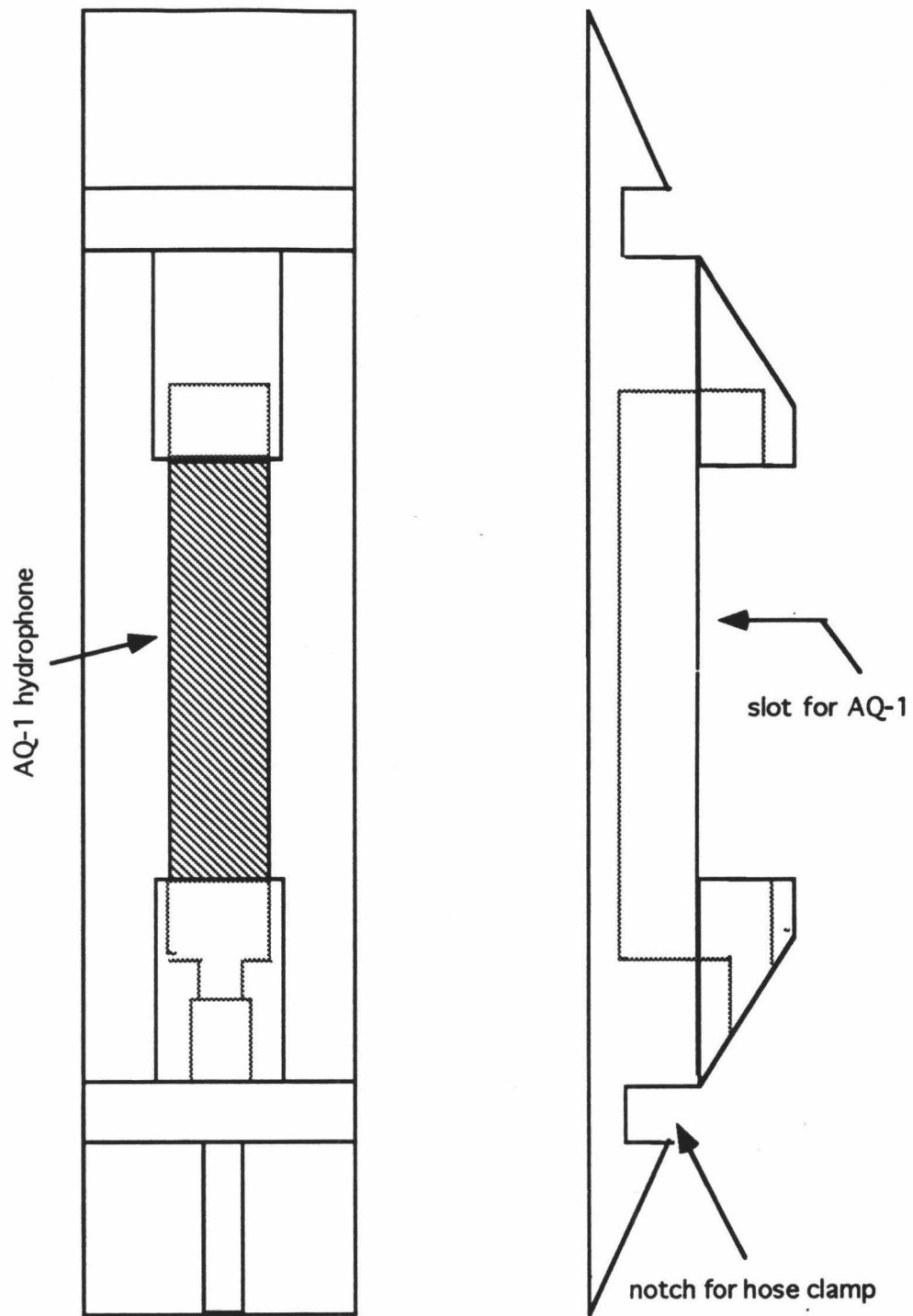


Figure 5. The holder for the AQ-1 Hydrophone

Acoustic Background

Seafloor sediments may be thought of as a two-phase composite material, consisting of granular solids and pore fluids (Ogushwitz, 1985c). They are regarded as a uniform material in physical model calculations and in most lab measurements. These two-phase uniform materials, however, are hard to find in the field, especially in shallow water environments where sediments may be poorly winnowed with larger skeletal fragments and other larger grains randomly distributed in fine sediments. This is a major source of the scatter in velocity measurement, because the waveform of the first arrival may be distorted and its coda may be longer owing to nonuniformity of the sediments.

Intrinsic attenuation is the energy loss due to frictional dissipation of elastic energy into heat. The mechanism of acoustic attenuation in a sediment is complex and still not well understood. Hamilton (1987) and Stoll (1985) provide recent reviews. The center of the debate is concentrated on the linear or nonlinear relationship between frequency and attenuation. The approach followed by Hamilton concludes that the attenuation coefficient is proportional to the first power of frequency (Hamilton 1974, 1980). This approach is entirely empirical but has been extremely effective (Kibblewhite, 1989). Hamilton explained his empirical result by using a viscoelastic model. It assumes that sediments can be represented by an isotropic two-phase system composed of sediment grains and water. The attenuation mechanism is based on the provision of velocity dispersion. When energy losses are small, attenuation can be regarded as linear with frequency. An alternative approach developed by Stoll and others (Stoll 1985, McCann and McCann 1969), assumes that two key mechanisms control the attenuation in marine sediments: the damping inherent in the sediment frame and the viscous action of the fluid motion relative to the frame. New experiments have shown that a third mechanism which results from local fluid motion in the vicinity of intergranular contacts may also be important at low frequency (Spencer, 1980; Stoll, 1985). Attenuation

should thus vary in a complex manner when all mechanisms are combined and show a nonlinear relation to frequency at f^1 , f^2 , or $f^{1/2}$, depending on the frequency range involved.

Attenuation measurement in situ is much more difficult than velocity measurement. The main requirements for attenuation measurement by Lance are: 1) All receivers must have the same frequency response or at least be calibrated correctly. 2) There must be limited distortion in the waveforms of received signals. Therefore, energy losses must be small and scattering negligible.

Signal Analysis and Data Processing

As mentioned above, Lance has ten channels sampled at 100 kHz. The full waveforms of the received signals are recorded in order to invert for velocity and attenuation. Velocity is usually determined in the time domain, and attenuation, which is related to energy loss, is measured in the frequency domain.

Biot (1956, 1962) devised a theoretical model of the acoustic behavior of a porous, saturated sediment. The model predicts that there are two kinds of compressional waves in porous, saturated sediments. The first kind of compressional wave is the compressional wave usually observed in sediments. The second wave, which has a very low velocity and high attenuation, has been observed and measured (Plona, 1980) only in man-made material at a frequency of 500 kHz. Only Biot's first wave has significance for wave propagation in marine sediments.

After corrections for geometric spreading, the amplitude of a body wave in sediment can be expressed as the $p_0 e^{-\alpha x}$, where α is the attenuation coefficient, proportional to the first power of frequency, and x is the distance. The quality factor Q is another parameter frequently used in the literature to designate attenuation characteristics of materials. Attenuation and Q are related by:

$$\alpha = \pi f / Qc, \quad (1)$$

where f is frequency and c is velocity. It can be seen that if the attenuation coefficient is proportional to the first power of frequency, then Q is independent of frequency.

Johnston and Toksoz (1981) present various definitions of Q and their interrelationships. A definition that relates Q to the wave amplitude A is given by:

$$1/Q = (1/\pi) (\Delta A/A), \quad (2)$$

where ΔA is the amplitude loss per cycle. O'Connell and Budiansky (1978) suggested a definition in terms of the mean stored energy W and the energy loss ΔW , during a single cycle of sinusoidal deformation:

$$Q = (4\pi W) / (\Delta W). \quad (3)$$

When this definition is used, Q is related to the phase angle, δ , between stress and strain:

$$1/Q = \tan \delta. \quad (4)$$

O'Connell and Budiansky (1978) also define Q in terms of complex phase velocity, $c(\omega)$, by

$$Q(\omega) = \text{Re}[1/c^2(\omega)] / \text{Im}[1/c^2(\omega)]. \quad (5)$$

This definition is nearly equivalent to the definition (2) of Johnston and Toksoz.

Frequency independent Q implies that the loss per cycle is independent of the time scale of oscillation. Kjartansson (1979) gives a linear description of attenuation with Q exactly independent of frequency. Kjartansson's model requires the phase velocity to be slightly dependent on frequency, but does not require any frequency cut-off.

Both Hamilton's viscoelastic model and Kjartansson's model assume that the attenuation mechanism is based on the principle of velocity dispersion. They have derived nearly identical relations of Q being independent of frequency with different methods and approximations. Many seismic in situ measurements have indicated that quality factor Q is effectively frequency independent in the seismic band (Kanamori & Anderson 1977).

Kibblewhite (1989) examined attenuation of sound in marine sediments through a review of the relevant literature from rock mechanics and underwater acoustics. He concluded that in spite of the sparsity of data for marine sediments at low frequencies, the widely held assumption that the relationship between attenuation and frequency is linear from seismic to ultrasonic frequencies does not appear justified. Nevertheless, Q is regarded as independent of frequency in our signal analysis procedure. Figure 6 shows block diagram of our signal processing procedure.

Velocity Data

Velocity results are obtained using the measured travel time difference between two receivers with known distance:

$$c = \Delta L / \Delta t .$$

where c is velocity, receiver separation is ΔL , and Δt is the travel time. Calibration of the acoustic path ΔL is indispensable in velocity measurements. It can be done in two ways. We may hang Lance in water and measure the travel time of every pair of receivers. If we have an underwater velocity meter, the accurate velocity of water will be known and the acoustic separation of every pair of receivers will be determined. In the absence of an underwater velocity meter we measure the distance from the top receiver

Signal Analysis and Data Processing

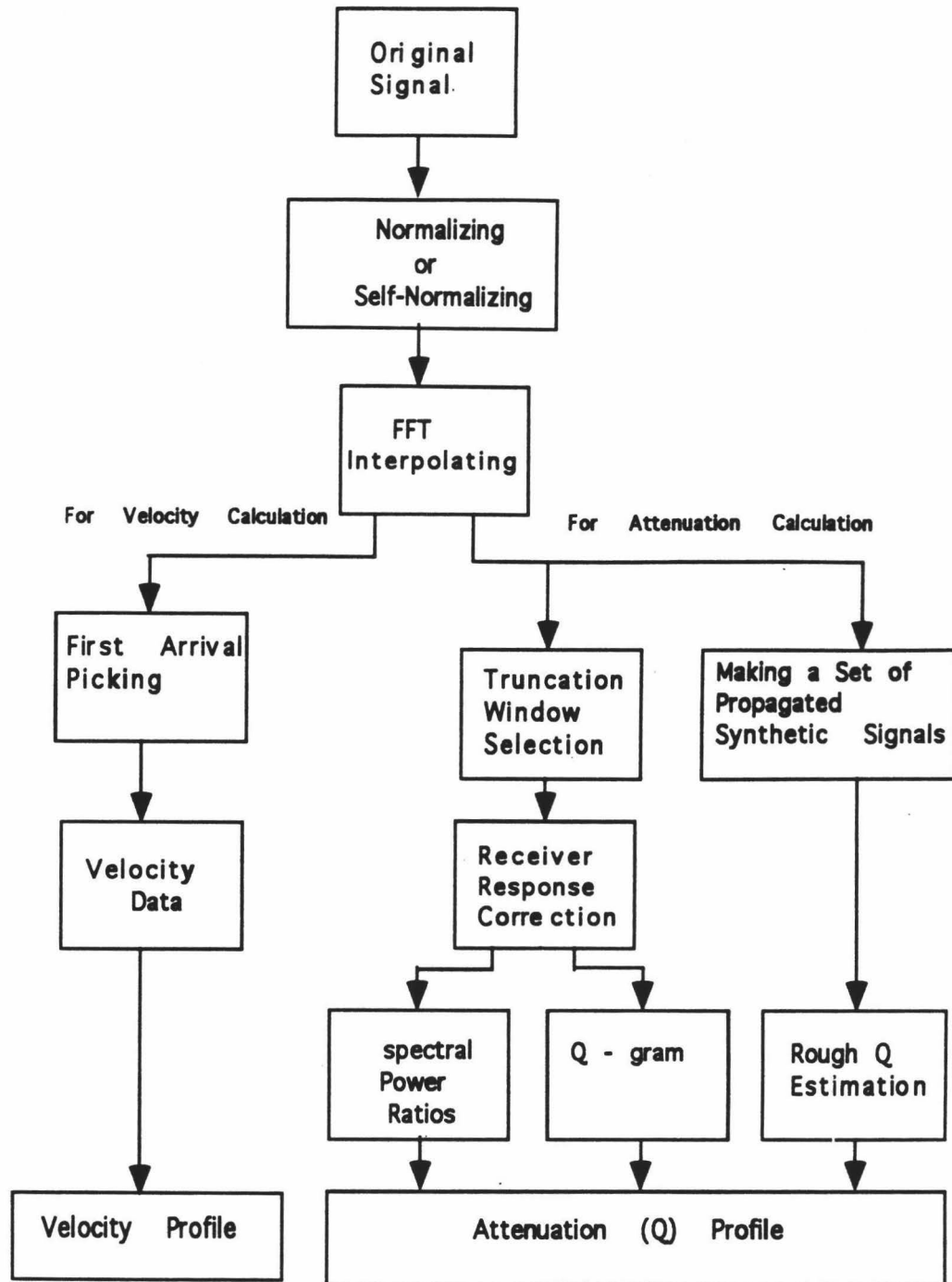


Figure 6. The procedure block diagram of signal processing

to the bottom receiver (which may be 5m to 10 m) as accurately as possible. We calculate the velocity of water by using this distance as the acoustic path. Then the acoustic path of every pair of receivers is determined using the calculated water velocity. A longer acoustic path will decrease the error in velocity as well as the error in the calibration of the acoustic path of every pair of receivers. For example, suppose the distance between the first receiver and the last receiver is 5 m and the error of measurement is 1 cm. The error this produces in the calculated distance between a pair of receivers with actual separation 0.5 m is about 1 mm or 0.2%. We assume that the acoustic path is the same in the water as it is in the sediment.

The precision of measurement of both velocity and attenuation is extremely sensitive to the sampling rate of the A/D converter. The A/D converters in Lance sample at 100 kHz, i.e with a 10 μ s in sampling interval. This rate is not quite high enough for sufficient precision in our adjacent-receiver acoustic path of 0.5 m. Ten μ s resolution leads to a precision in velocity of about 40-60 m/s (2.5%-4.0%). Our aim for the velocity resolution of Lance is that the largest uncertainty in velocity must be lower than 1% of the expected velocity. This problem is addressed by producing an interpolated waveform with a spectrum identical to that of the original waveform. The original waveform is transformed from the time domain to the frequency domain by Fourier transform. The Nyquist frequency of Lance's signals is 50 kHz. We extend the frequency range of the original waveform from 50 kHz to 200 kHz by adding zero values in the spectrum from 50 kHz to 200 kHz. An interpolated waveform is obtained from the new spectrum by inverse Fourier transform. Figure 7 shows an original and interpolated signal. Although an interpolated waveform does not carry more information than the original waveform, the accuracy of the computer arrival time picking procedure is thereby improved from 10 μ s to 2.5 μ s.

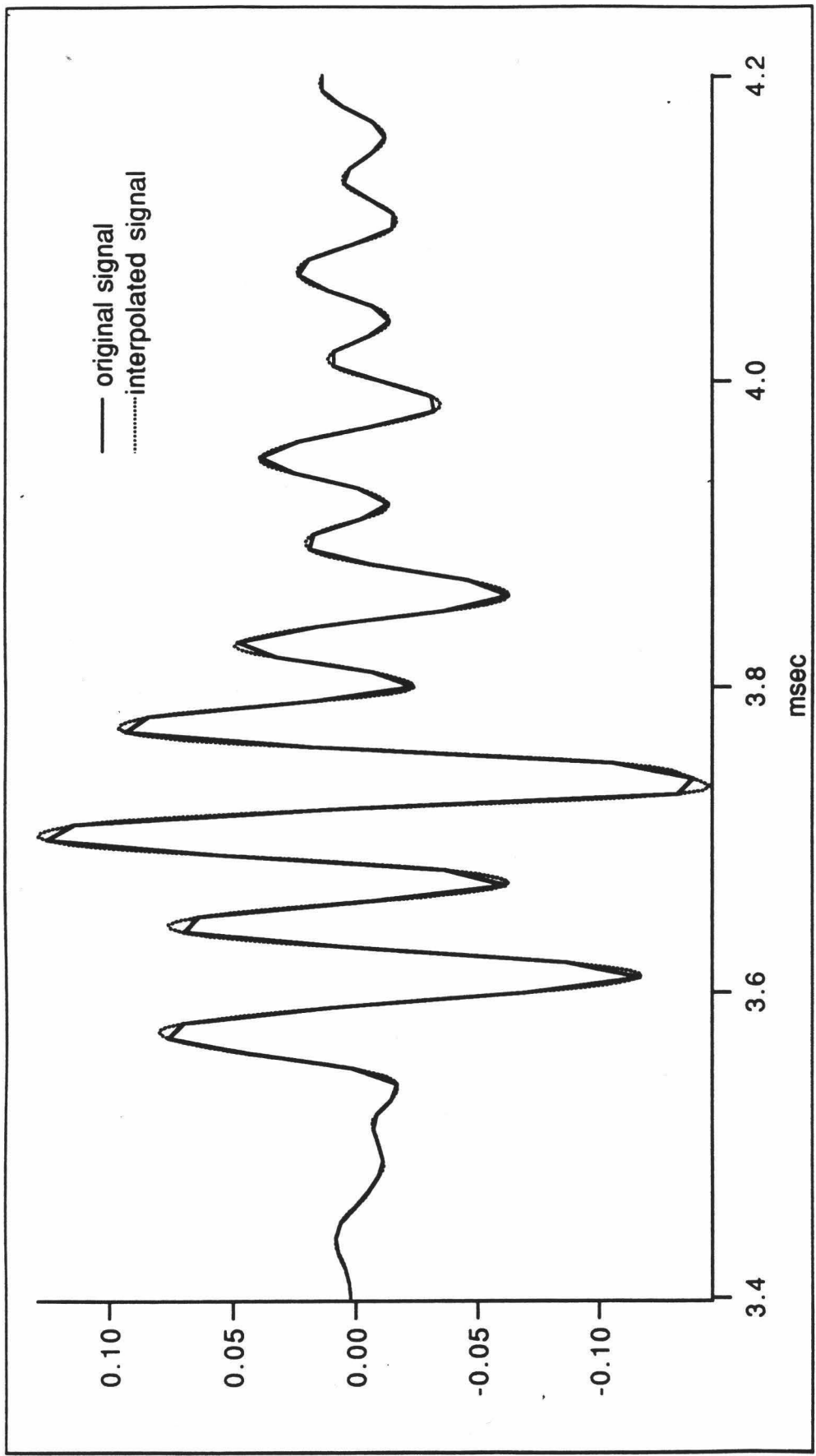


Figure 7 The original signal and interpolated signal

If the sediments are heterogeneous, as with poorly winnowed shelf sediments, the waveforms of received signals may be distorted due to multiple arrivals caused by scatter. This situation makes it harder to detect the first arrival for velocity calculation and thus lowers the precision of velocity measurements. Figure 8 compares received signals of relatively uniform deep-sea sediment (signals with impulsive first arrivals) with those from shallow water shelf sediments rich in skeletal fragments (signals with emergent first arrivals). The distorted waveform does not allow us to figure out the delay time for velocity calculation by picking later arrivals if the first arrival is not apparent (Fig. 9).

Attenuation Data

Attenuation measured from field data is termed effective attenuation because it includes the contributions of both intrinsic and apparent attenuation. Three key mechanisms - damping inherent in the sediment frame, viscous action of fluid motion relative to frame, and local fluid motion in the vicinity of intergranular contacts - control intrinsic attenuation in different frequency bands (Stoll, 1985; McCann and McCann, 1969; Spencer, 1980). Energy is removed from the coda (into heat) in intrinsic attenuation. Apparent attenuation is the body wave decay in amplitude resulting from the scattering of energy by a heterogeneous medium. It removes energy from the initial pulse and adds that energy to the coda. If apparent attenuation is much smaller than intrinsic attenuation, then effective attenuation is given approximately by the relation: $\alpha_e = \alpha_a + \alpha_i$ with obvious definitions for α_e , α_a and α_i .

Methods to Estimate Q

Spectral ratios

The spectral ratio method has been used by several investigators to determine compressional and shear Q in marine sediments (Jannsen et al., 1985; Jacobson 1987; Bromirski, 1992a). It estimates the Q factor by using the ratio of amplitude spectra of different arrivals. Assume two signals $S_1(t)$ and $S_2(t)$ received from a pair of receivers

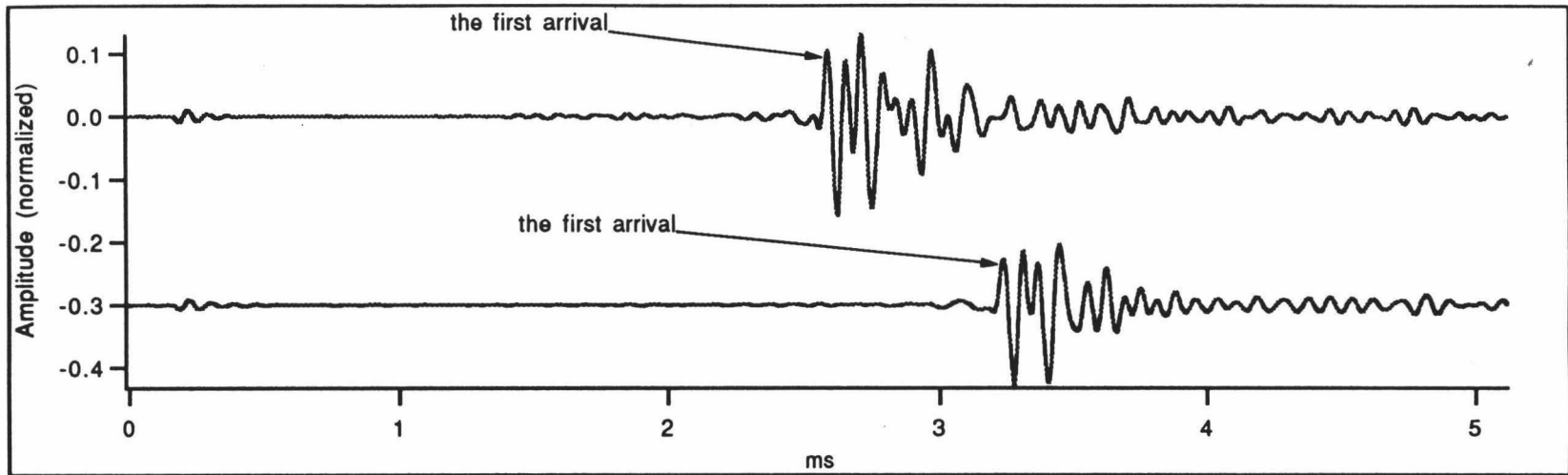


Figure 8A. The waveform of signal received in deep water.
It shows an impulsive first arrival.

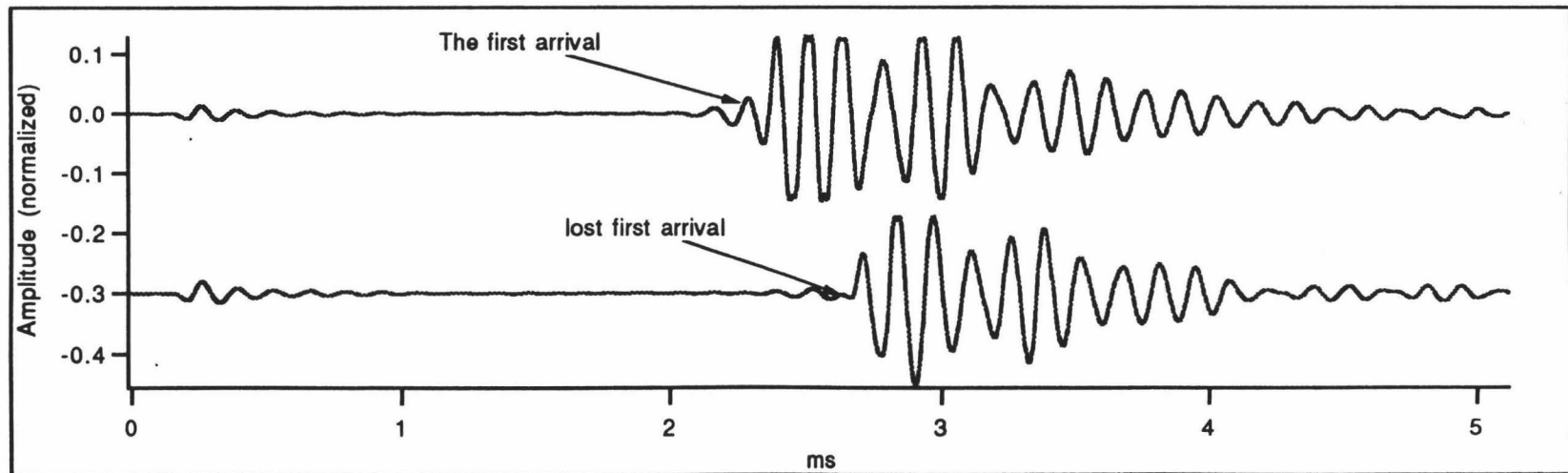


Figure 8B. The waveform of signal received in shallow water.
It shows an emergent first arrival.

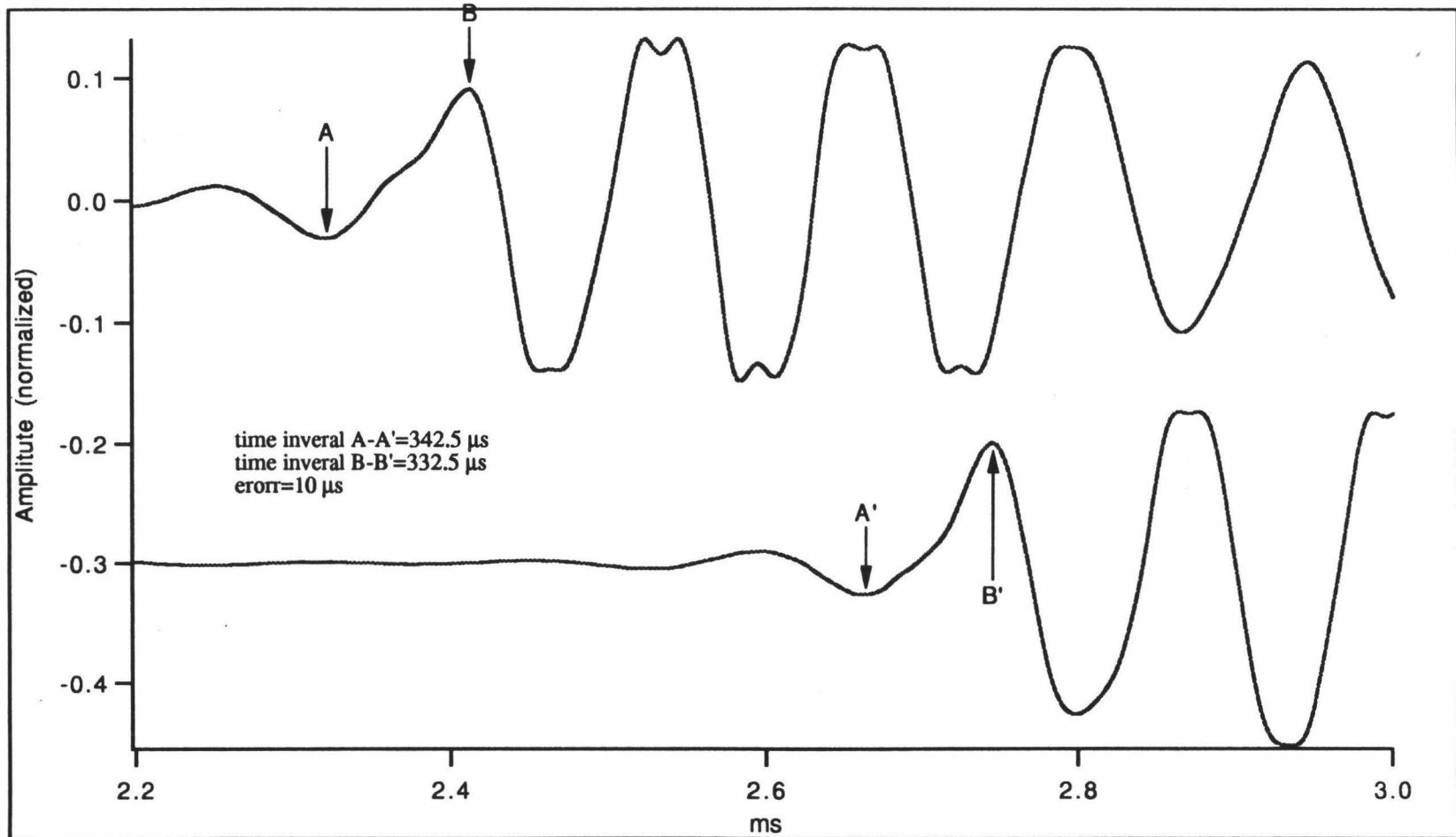


Figure 9. The traveltime error caused by distorted waveform. Waveform distortion causes a 10 μ s disagreement between A-A' and B-B'.

R_1 and R_2 with separation x . $S_1(\omega)$ and $S_2(\omega)$ are the amplitude spectra of $S_1(t)$ and $S_2(t)$ respectively. The amplitude spectrum of $S_2(\omega)$ is related to $S_1(\omega)$ by :

$$|S_2(\omega)| = |S_1(\omega)| \mathfrak{S} \mathfrak{R} \exp [-\alpha x] \quad (6)$$

where \mathfrak{S} is a ratio of geometrical spreading terms and \mathfrak{R} contains reflection and transmission coefficients, all assumed independent of frequency. The attenuation coefficient is α and ω is the angular frequency. Taking the natural log of the the ratio of two spectra gives:

$$\ln SR(\omega) = \ln |S_2(\omega) / S_1(\omega)| = \ln |\mathfrak{S} \mathfrak{R}| - \alpha x \quad (7)$$

Letting $x = \Delta t c$, where Δt is the travel time from R_1 to R_2 and c is average velocity over the interval x . gives:

$$\ln SR(\omega) = \text{const} - (\Delta t / 2) (Q^{-1}) \omega \quad (8)$$

in which const is a frequency independent term that includes spreading and transmission losses. Differentiating with respect to ω gives:

$$d[\ln SR(\omega)]/d\omega = -(\Delta t / 2) (Q^{-1}) \quad (9)$$

or with respect to frequency f

$$d[\ln SR(\omega)]/df = -(\pi \Delta t) (Q^{-1}) \quad (10)$$

If Q is independent of frequency f , equation (8) describes a straight line with slope $a_1 = -(\pi \Delta t) (Q^{-1})$. From the slope we can obtain a Q factor of effective attenuation:

$$Q = -(\pi \Delta t) / a_1 \quad (11)$$

Although equation (8) describes a straight line, for real signals the graph of $\ln SR$ may be a jagged curve due to contamination by noise, interference from other waves, uncertainty in spectral estimates, and differences among the response functions of receivers. The slope a_1 is determined by a least-squares fit to $\ln SR$ (Fig. 10).

The received signals may contain extra arrivals. In the Lance measurement, the extra arrivals probably result from reflection off the mechanical structure of Lance. In practice, signals are truncated to remove these extra arrivals. Truncation, however, usually affects the wave spectra, particularly when the removed parts still contain a significant portion of the signal. The length of truncation windows selected for the spectral ratio method can significantly affect the Q estimate. We used synthetically propagated signals to test for the best truncation window length as follow.

Assume that a measured reference signal at x_1 has a spectrum $S_0(\omega)$. Then, in theory, the signal measured at x_2 should have spectrum given by :

$$S_s(\omega) = S_0(\omega)\exp(i\omega x/c_0)\exp[-(\omega x)/(c_0Q)] , \quad (12)$$

where $x=x_2-x_1$ is the distance of propagation, and c_0 is the real part of complex velocity c . We refer to $S_s(\omega)$ as the synthetically propagated signal, or simply synthetic signal. The term $\exp(i\omega x/c_0)$ represents the time delay and $\exp[-(\omega x)/(c_0Q)]$ represents the attenuation of the synthetic signal. We obtain a time domain synthetic signal $S_s(t)$ by applying an inverse Fourier transform to $S_s(\omega)$. We used different truncation window lengths to calculate the Q of synthetic signals with formula (11). An optimal truncation window length is obtained when the Q calculated from the synthetic signal equals the actual Q value used in the synthetic propagation by equation (12). The most significant portion of the signal is included in this window. The length of the truncation window may vary with different types of sediments. Figure 11 shows the Q values estimated

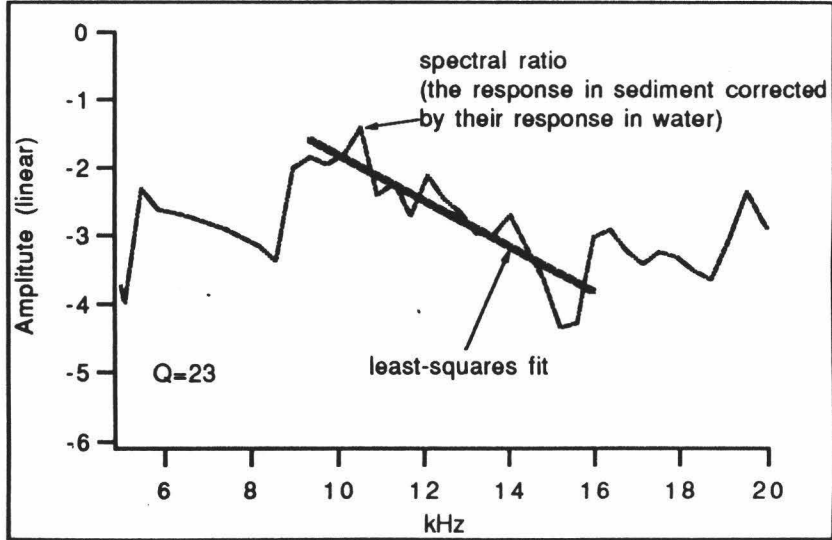
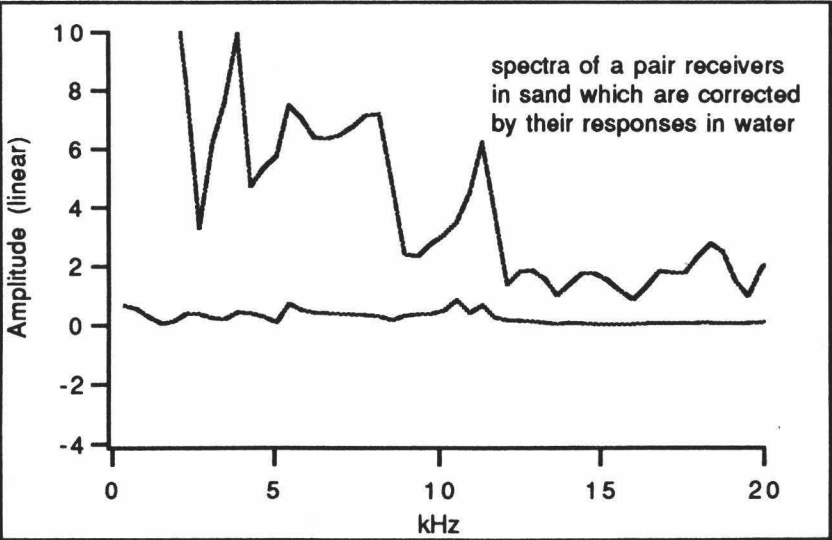
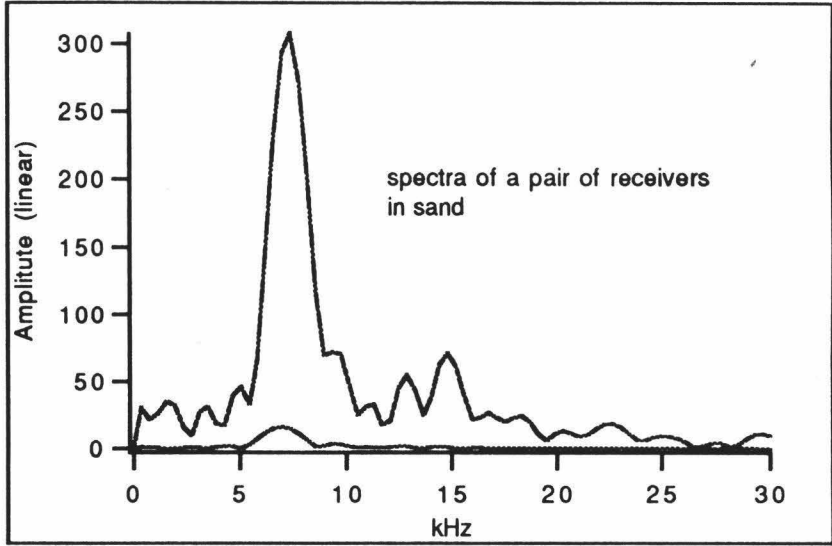
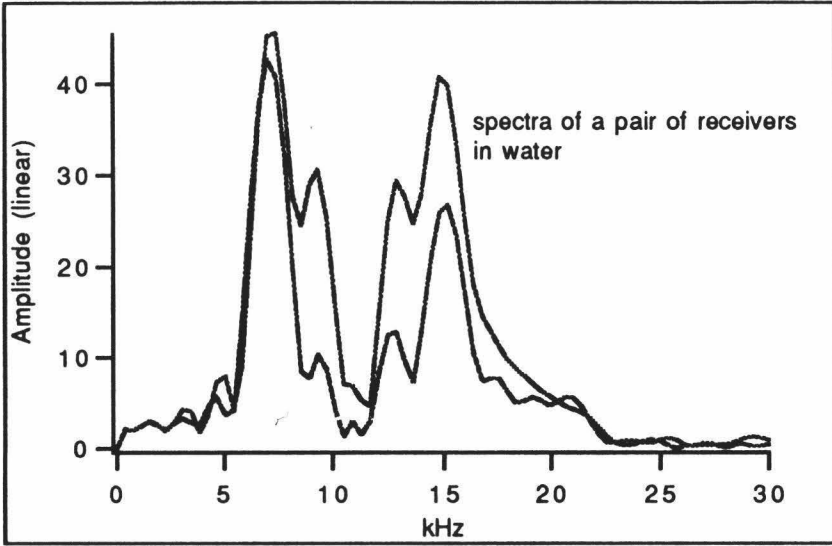


Figure 10. Determination of Q by power spectral ratio.
Spectral units are linear.

with different windows. Several tests of truncation window length indicated that for fine pelagic sediments a 640 μ s window is suitable for Lance signals.

Subsequently we included the effects of velocity dispersion in our synthetic tests. Bromirski et al (1993) derived a wave propagator $\vartheta(\omega)$ from Kjartansson's (1979) model of constant-Q complex velocity, $c(\omega)$, given by:

$$c(\omega) = c_0 [(-i \omega) / \omega_0]^\gamma , \quad (13)$$

where $\omega_0 = 2\pi f_0$, with f_0 the reference frequency and c_0 the phase velocity at $Q=\infty$. The Q dependence appears in γ , defined by $\gamma = (1/\pi) \tan^{-1} (1/Q)$. Then

$$\vartheta(\omega) = \exp \{ i\omega\Delta t | \omega_0/\omega |^\gamma [1 + i \tan (\pi \gamma/2)] \} . \quad (14)$$

The spectrum of the synthetic signal $S_s(\omega)$ becomes:

$$S_s(\omega) = S_0(\omega)\vartheta(\omega) = S_0(\omega)\exp \{ i\omega\Delta t | \omega_0/\omega |^\gamma [1 + i \tan (\pi \gamma/2)] \} . \quad (15)$$

The results show that there is little difference between spectral ratios from the synthetic signals calculated using equation (12) versus those calculated using equation (15) (Fig. 12). When $Q > 20$, velocity dispersion in the Lance frequency band does not significantly affect Q computation.

The main difficulty in our application of the spectral ratio method is the variability in the receiver response function. To see this, notice that the receiver response function cancels out of the spectral ratio in equation (7) only if the response of receiver 1 is identical to the response of receiver 2.

Calibration of Lance in water may be used to reduce the error in attenuation measurements caused by the non-identity of receiver response functions. Our method for this, outlined below, is based on the assumption that, although the response function of every receiver is different, each is the same in the sediments as it is in the water. In this

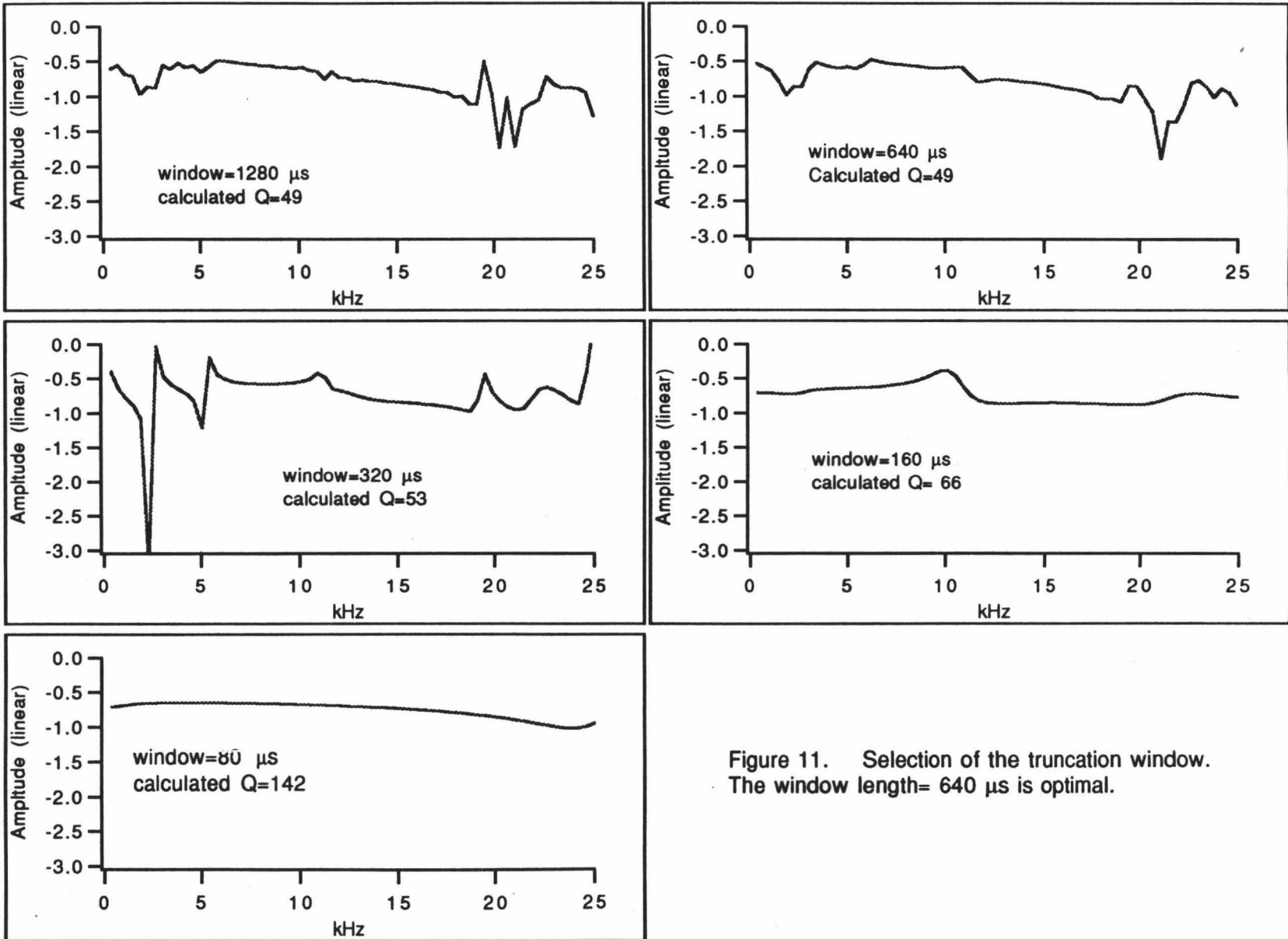


Figure 11. Selection of the truncation window. The window length= 640 μ s is optimal.

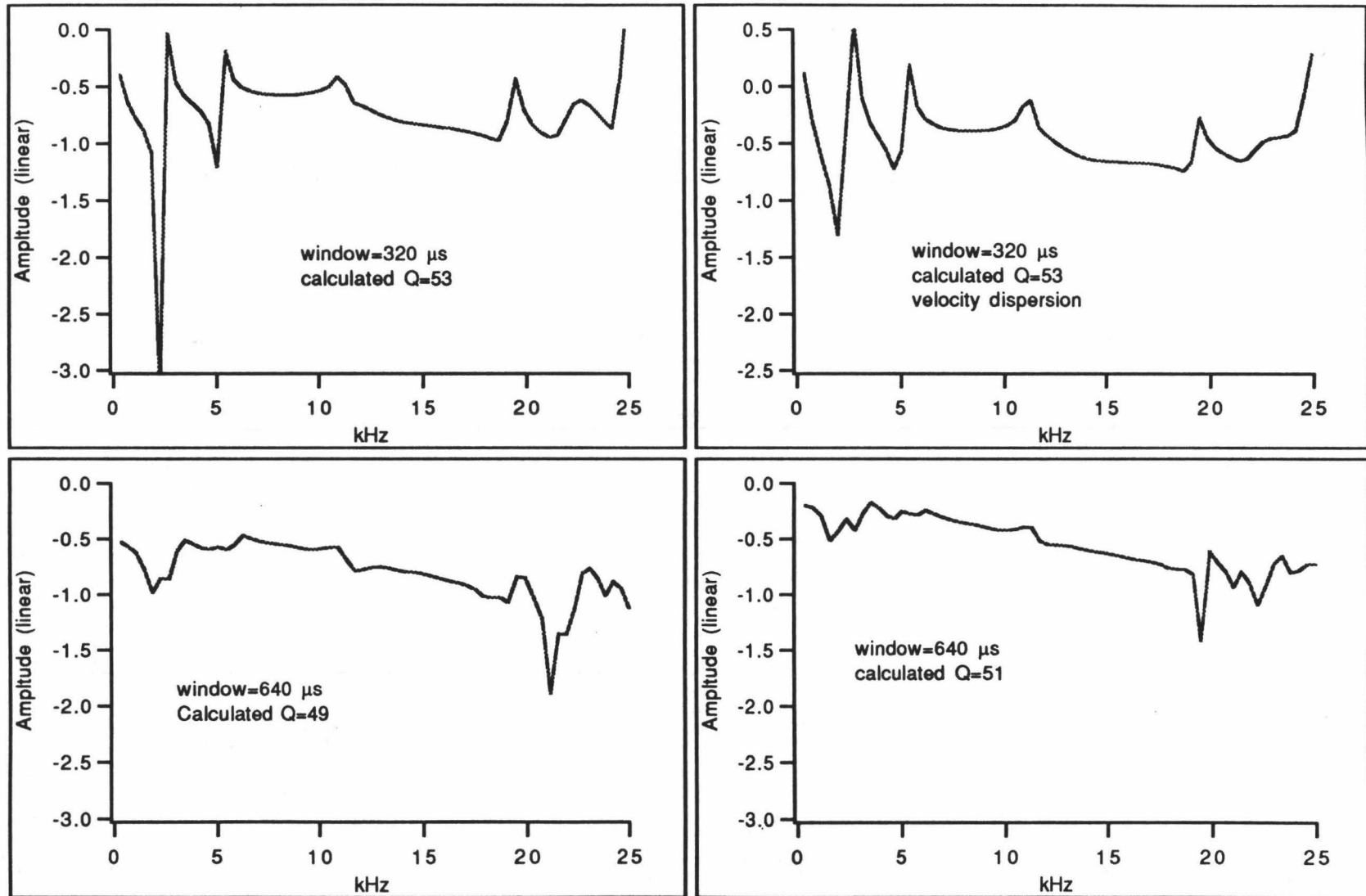


Figure 12. Comparison of spectral ratios with and without velocity dispersion. There is not a significant difference between them.

assumption, the variation of the response functions with the acoustic load impedance of the receiver is ignored.

To implement the method, Lance is fired once in the water and once in the sediment. Suppose that signals $W_1(\omega)$ and $W_2(\omega)$ are received from a pair of receivers R1 and R2 in the water, and that signals $S_1(\omega)$ and $S_2(\omega)$ are received from the same pair of receivers in the sediment. Let the response functions of R1 and R2 be $R_1(\omega)$, $R_2(\omega)$. Then the spectra of the recorded signals can be expressed as:

$$\begin{aligned}
 W_1(\omega) &= w_1(\omega) R_1(\omega) \\
 W_2(\omega) &= w_2(\omega) R_2(\omega) \\
 S_1(\omega) &= s_1(\omega) R_1(\omega) \\
 S_2(\omega) &= s_2(\omega) R_2(\omega) .
 \end{aligned}
 \tag{16}$$

where $s_1(\omega)$ and $s_2(\omega)$ are the true signals in the sediment, $w_1(\omega)$ and $w_2(\omega)$ are the true signals in the water. Equation (16) uses the assumption that each receiver is the same in the sediments as it is in the water. For use below, note that

$$\begin{aligned}
 W_1/W_2 &= [w_1/w_2][R_1/R_2] \\
 S_1/S_2 &= [s_1/s_2][R_1/R_2] .
 \end{aligned}
 \tag{17}$$

In the water Q is essentially infinite ($>20,000$), so the only differences between the true water signals $w_1(\omega)$ and $w_2(\omega)$ are due to spreading. Here we make a second assumption that $w_1(\omega)/w_2(\omega) = a_{12}$ is independent of frequency ω . With this assumption we have

$$R_1/R_2 = [W_1/W_2] [1/a_{12}] .
 \tag{18}$$

Therefore

$$[S_1/W_1]/[S_2/W_2] = [s_1/s_2] [1/a_{12}] .
 \tag{19}$$

Hence

$$\ln[(S_1/W_1)/(S_2/W_2)] = \ln [s_1/s_2] - \ln |a_{12}| . \quad (20)$$

Substituting equation (8) into (20) gives:

$$\ln[(S_1/W_1)/(S_2/W_2)] = \text{const} - (\Delta t / 2) (Q^{-1}) \omega . \quad (21)$$

If Q is independent of frequency then equation (21) (similar to equation (8)), describes a straight line with slope $a_1 = -(\pi\Delta t)(Q^{-1})$. The difference between equations (8) and (21) is only in the constant term.

Q-gram

Noise and signal clipping often affect field data, and both phenomena may be expected to distort signal spectra. Bromirski et al. (1992a, 1992b, 1993) present the Q-gram method to estimate Q directly from pulse width in the time domain. An advantage of the Q-gram method over other methods is that it is relatively robust with regard to noise, phase changes, and signal clipping.

The pulse width of an acoustic signal increases monotonically with distance and with Q^{-1} when it propagates in sediments. Bromirski et al. (1992a, 1994) define propagation loss Ψ as:

$$\Psi (\tau_1, \tau_2) = (\tau_2 - \tau_1) / \Delta t \quad (22)$$

where τ_1 and τ_2 are the coda pulsewidths of a signal recorded from receivers R1 and R2 respectively. Let the measured travelttime from R1 to R2 be Δt . Then the coda pulse width τ is defined as:

$$\tau = [1 / \int_{t_1} |\sigma(t)|^2 dt] [\int_{t_1} \tau(t) |\sigma(t)|^2 dt] , \quad (23)$$

where $\tau(t)$ is the instantaneous pulse width (defined below) and $\sigma(t)$ is the instantaneous amplitude. From the wavelet, $s(t)$, and its Hilbert transform, $s^\wedge(t)$, we obtain the instantaneous amplitude $|\sigma(t)|$ given by:

$$|\sigma(t)| = [s(t)^2 + s^\wedge(t)^2]^{1/2} \quad , \quad (24)$$

and the instantaneous phase $\phi(t)$, which must be unwrapped, from:

$$\phi(t) = \tan^{-1}[s^\wedge(t)/s(t)] \quad . \quad (25)$$

Then $\tau(t)$ is given by:

$$\tau(t) = [(1/2\pi) (d\phi(t)/dt)]^{-1} \quad . \quad (26)$$

From equations (22) - (26), and with measured Δt , we obtain the propagation loss Ψ .

Although Q is closely related to propagation loss Ψ , one can not obtain the Q of the data from equation (22) directly. It is necessary to construct a graph of Ψ versus Q^{-1} and use this graph to obtain the actual Q^{-1} of the data. The constructed graph of Ψ versus Q^{-1} is called the Q -gram.

To construct the Q -gram we proceed as follows. First we generate a set of synthetic wavelets for various values of Q^{-1} by using an actual signal $s_1(t)$ as a reference wavelet. Equation (12) or (15) is the formula of the spectrum of the synthetically propagated signal. The propagation loss Ψ' of every synthetic wavelet is then calculated. The Q -gram is the plot of synthetic propagation loss Ψ' between the reference and propagated wavelets, versus Q^{-1} . Once the Q -gram is constructed, we compute the propagation loss Ψ of the actual signal $s_2(t)$. The corresponding Q estimate is then obtain from the Q -gram by linear interpolation between the nearest values of Ψ' on the Q -gram. The procedure is more complicated than the spectral ratio method, because we have to construct a Q -gram for each pair of receivers in the Lance data.

As with spectral ratios, the non-identity of receiver response functions appears to be the main barrier in the Q-gram method. If the Q-gram of a pair of receivers is different from others at the same distance and velocity, the estimated Q will also be different.

The Q-gram method is potentially useful for processing Lance data if the non-identity of the receiver response function can be corrected for by a scheme such as the one outlined above.. In this paper, the method is introduced but is not applied to the Lance data processing.

Field Application

A comprehensive experiment was carried out on an Atlantic deep-water sediment pond, where P-wave velocity, wet-bulk density, grain density, porosity, and calcite content of recovered sediment samples were measured in the laboratory.

General Geological Description of the Field Area

The Lance experiment was located (Fig. 13) at a sediment pond on the west side flank of the Mid-Atlantic Ridge (MAR). The sediment pond is a deep, 470 km long bathymetric valley covered with soft, reddish-brown ooze. The two principal measurement sites are labeled A (Station #1 - Station #5) and B' (Station #6). Site B' lies at the west end of the sediment pond and the east end of Site A. Figures 14 and 15 show the bathymetry of Site A and Site B', respectively.

The surficial sediments of the sediment pond are dominantly calcareous ooze. A core (Core #1) recovered at Site A has an average calcium carbonate content of about 77%. Two photomicrographs of the core sample illustrate the texture of the sediments at Site A (Fig. 16) and Site B' (Fig. 17). A fine-scale geological and geophysical survey at sites A and B' (Tucholke, 1993) revealed that the crust is about 24-m.y. old at Site B' and 9

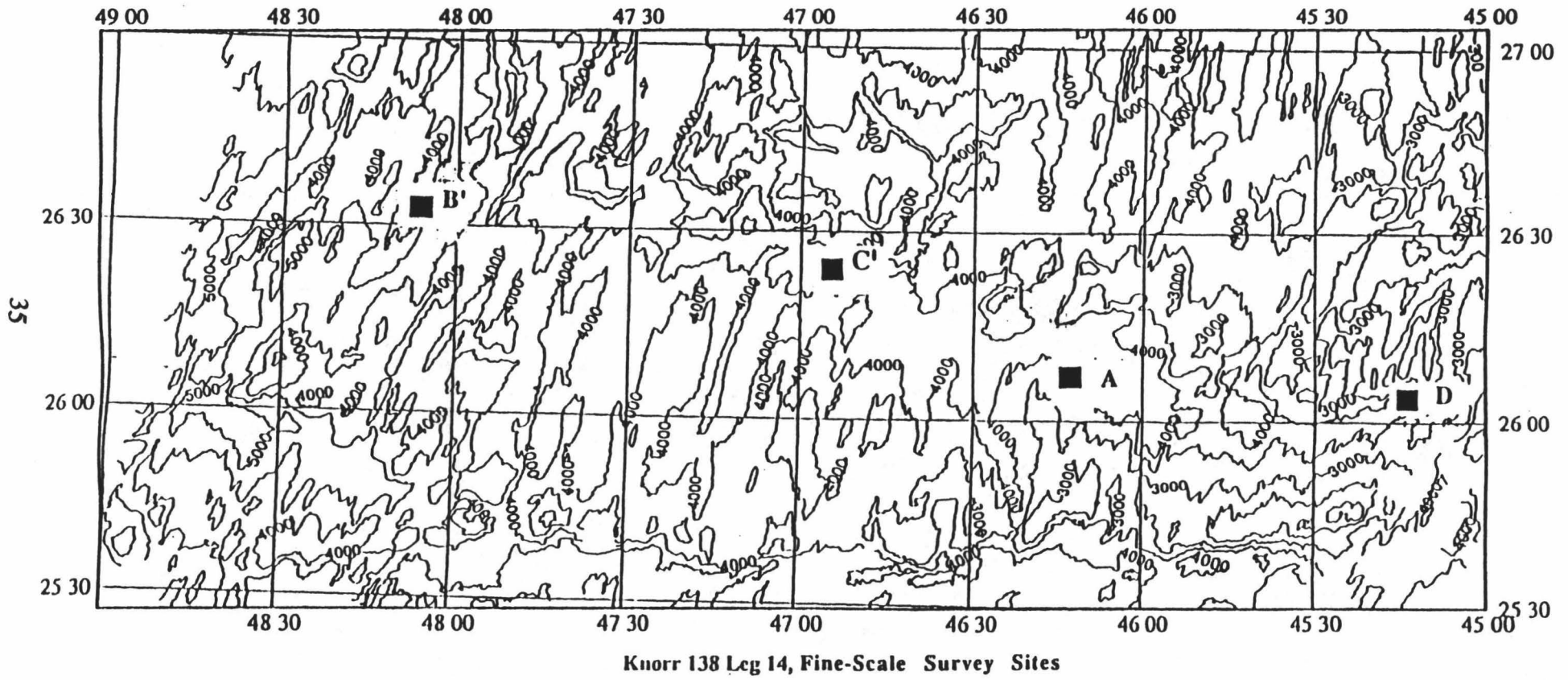


Figure 13. Bathymetry of the sediment pond on the west flank of the Mid-Atlantic Ridge
 (From Brian E. Tucholke et al)

Bathymetry Site A and D

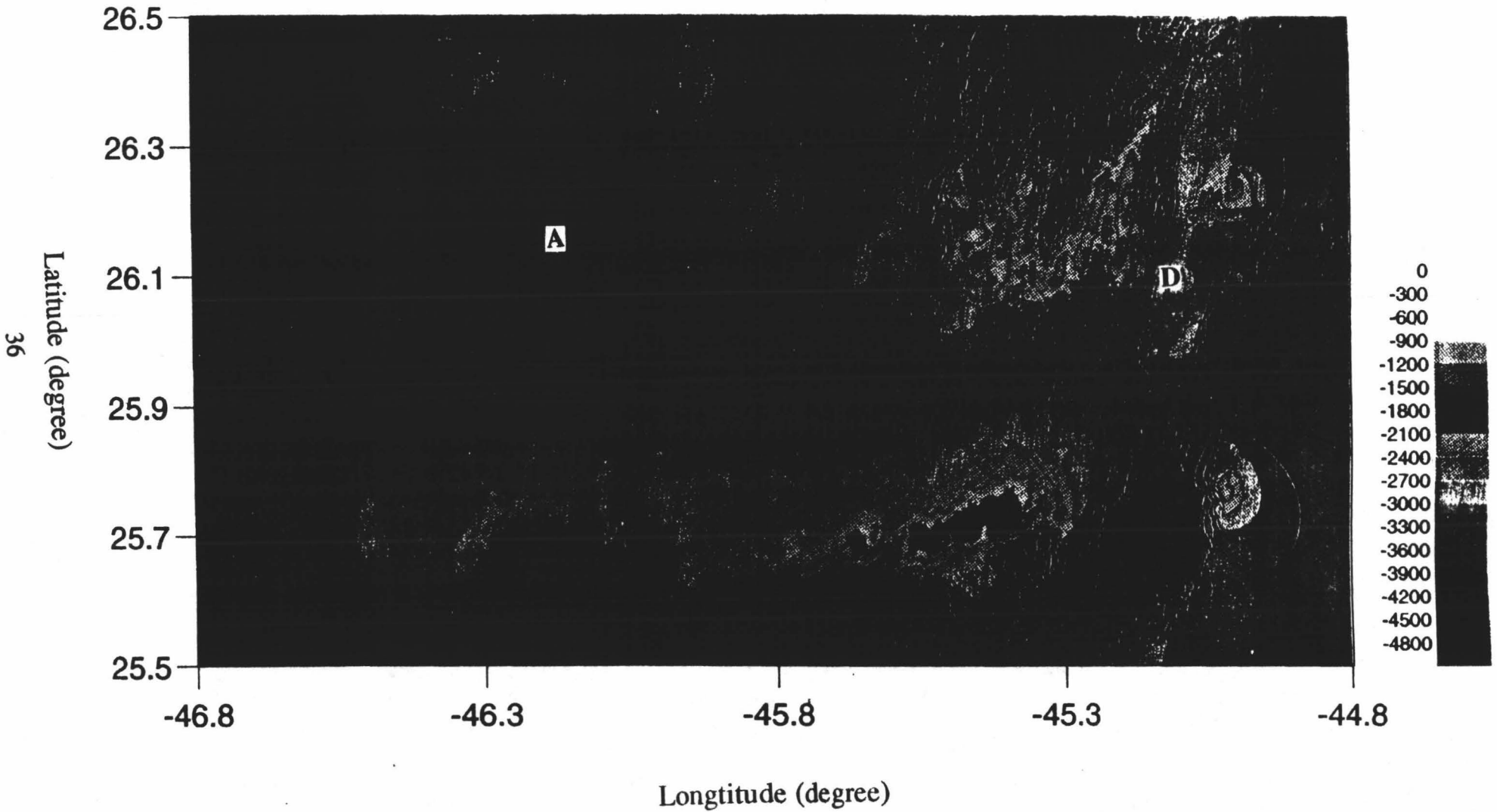


Figure 14. Bathymetry chart of Site A and Site D.

Bathymetry Site B' and C'

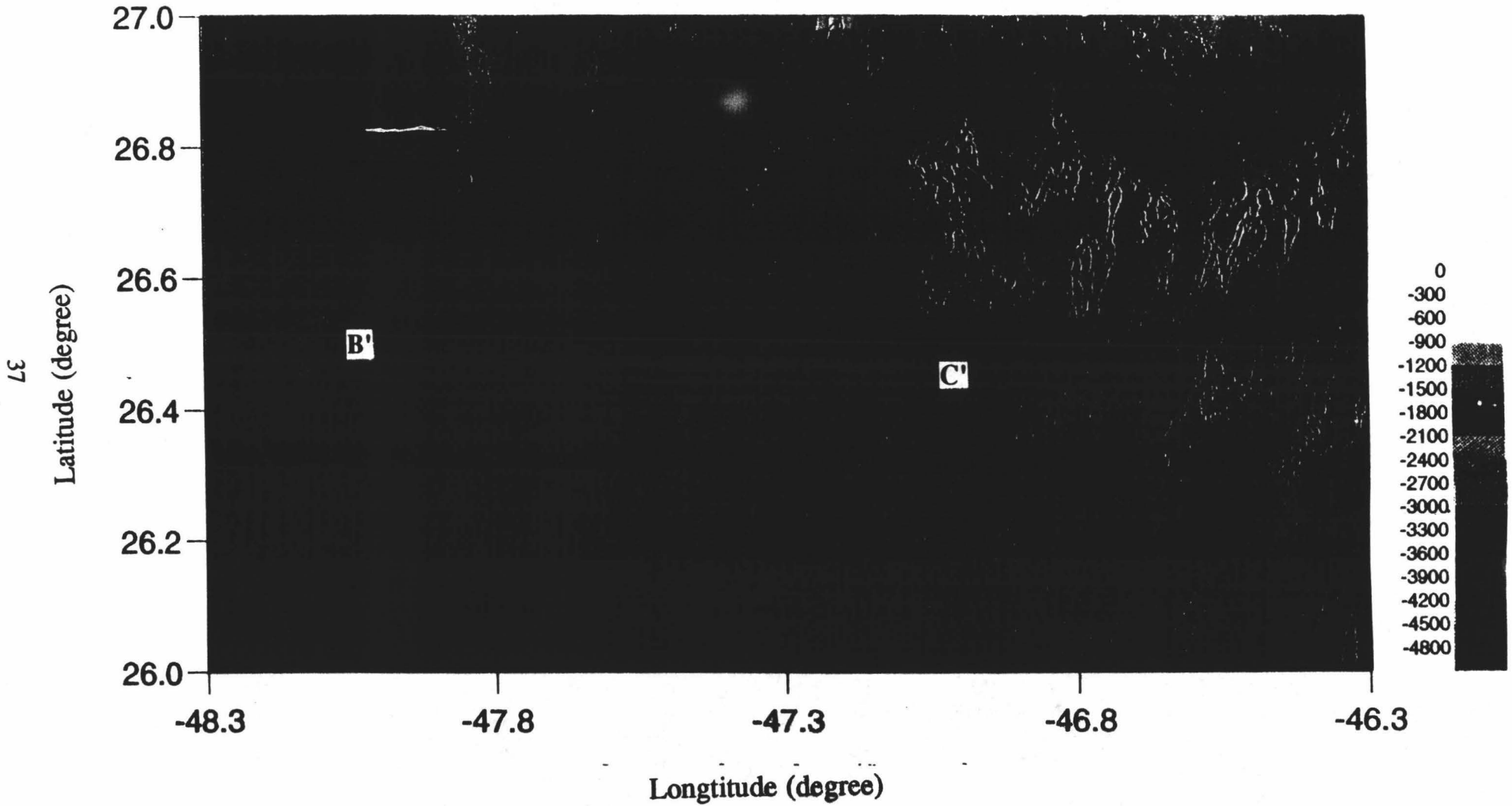


Figure 15. Bathymetry chart of Site B' and Site C'.

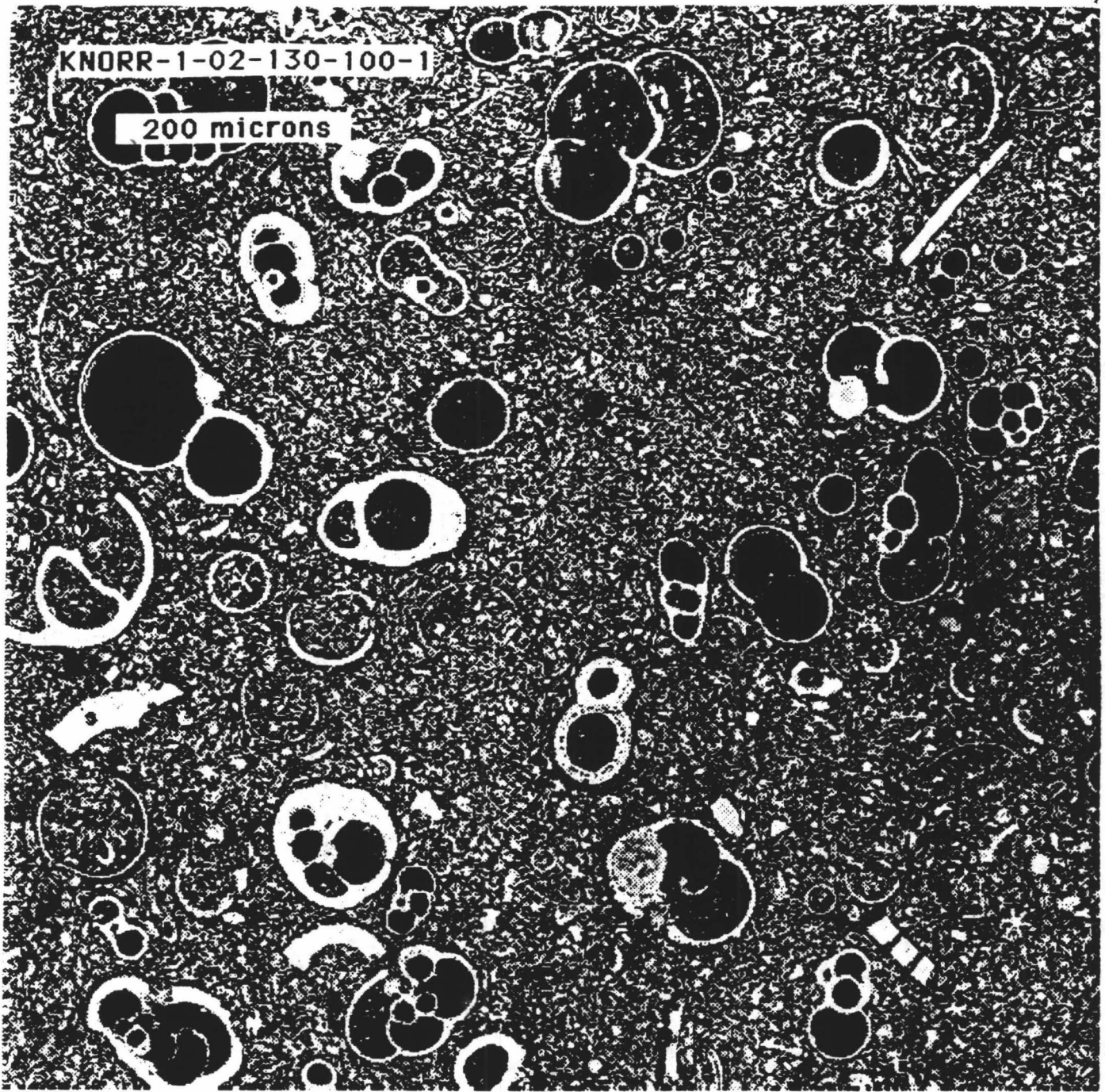


Figure 16. A photomicrograph of Core #1 sample (2.75 mbsf, in Site A).

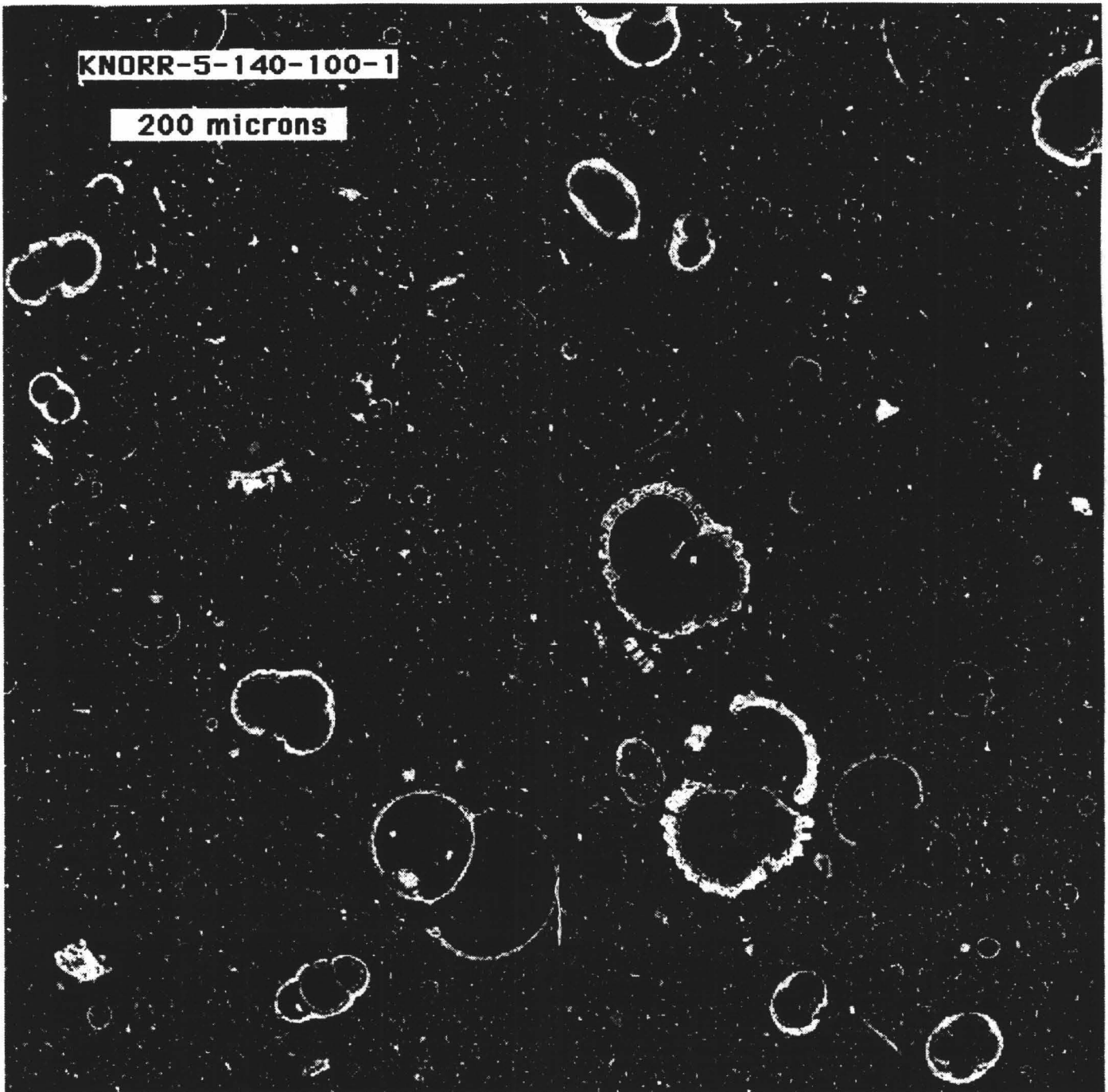


Figure 17. A photomicrograph of Core #5 sample (1.40 mbsf, in Site B').

-m.y. old at Site A, although the sediments of the two sites are comparable in visual observations.

Field Operation

Nine receivers were mounted on a gravity core or a metal heat flow probe, each about 5 m long. Good data were obtained from 6 stations in water depths from 4000 m to 5500 m. In one operation near the beginning of the experiment we tried to use plastic, larger size gravity corer pipes to collect the in situ data and recover samples.

Unfortunately, the plastic pipes split almost every time. We had no alternative but to use a metal, smaller size heat flow probe. This metal pipe perfectly penetrated the sediment layer, but was unable to recover sediment samples. An acoustic (12 kHz) pinger was mounted on the top of the gravity corer to indicate the down-going locus of Lance on a depth recorder.

Eight gravity core samples were recovered from the sediment pond (locations in Table 1). The good in situ Lance data were obtained on Station #1-Station #6 (see Table 1) with the metal pipe. Lance was working in multiple-measurement mode on each station. At Station #6, in a single lowering Lance penetrated into the sediment layer five times to record data. That is Lance recorded five independent data sets at one station. From Station #1-Station #5, Lance completed measurements at different five stations in one lowering. After completing the measurement at one station, Lance was raised to a position several hundred meters above the seafloor, and the ship towed Lance to the next station at a speed of 2 knots. After 5 measurements at 5 stations, which took about 12 hours, Lance was retrieved and the data from all 5 stations were transferred to the computer. The multiple-measurement mode saved considerable deployment time. Figure 18 shows the recorded waveforms from 5 stations (Station #1-Station #5) and Figure 19 shows that of a single station (Station #6).

Table 1. The locations of in situ measurements and coring

In situ measurements:

STATION	LATITUDE	LONGITUDE
Station #1	26° 07.352' N	46° 11.035' W
Station #2	26° 09.239' N	46° 09.433' W
Station #3	26° 10.487' N	46° 08.284' W
Station #4	26° 11.540' N	46° 07.176' W
Station #5	26° 11.992' N	46° 06.654' W
Station #6	26° 31.940' N	48° 00.778' W

Coring:

STATION	LATITUDE	LONGITUDE
Core #1	26° 07.889' N	46° 10.570' W
Core #2	26° 08.673' N	46° 09.671' W
Core #3	26° 10.173' N	46° 08.570' W
Core #4	26° 15.641' N	46° 33.628' W
Core #5	26° 31.317' N	48° 01.409' W
Core #6	26° 20.596' N	46° 45.522' W
Core #7	26° 23.533' N	46° 58.819' W
Core #8	26° 27.219' N	47° 24.426' W

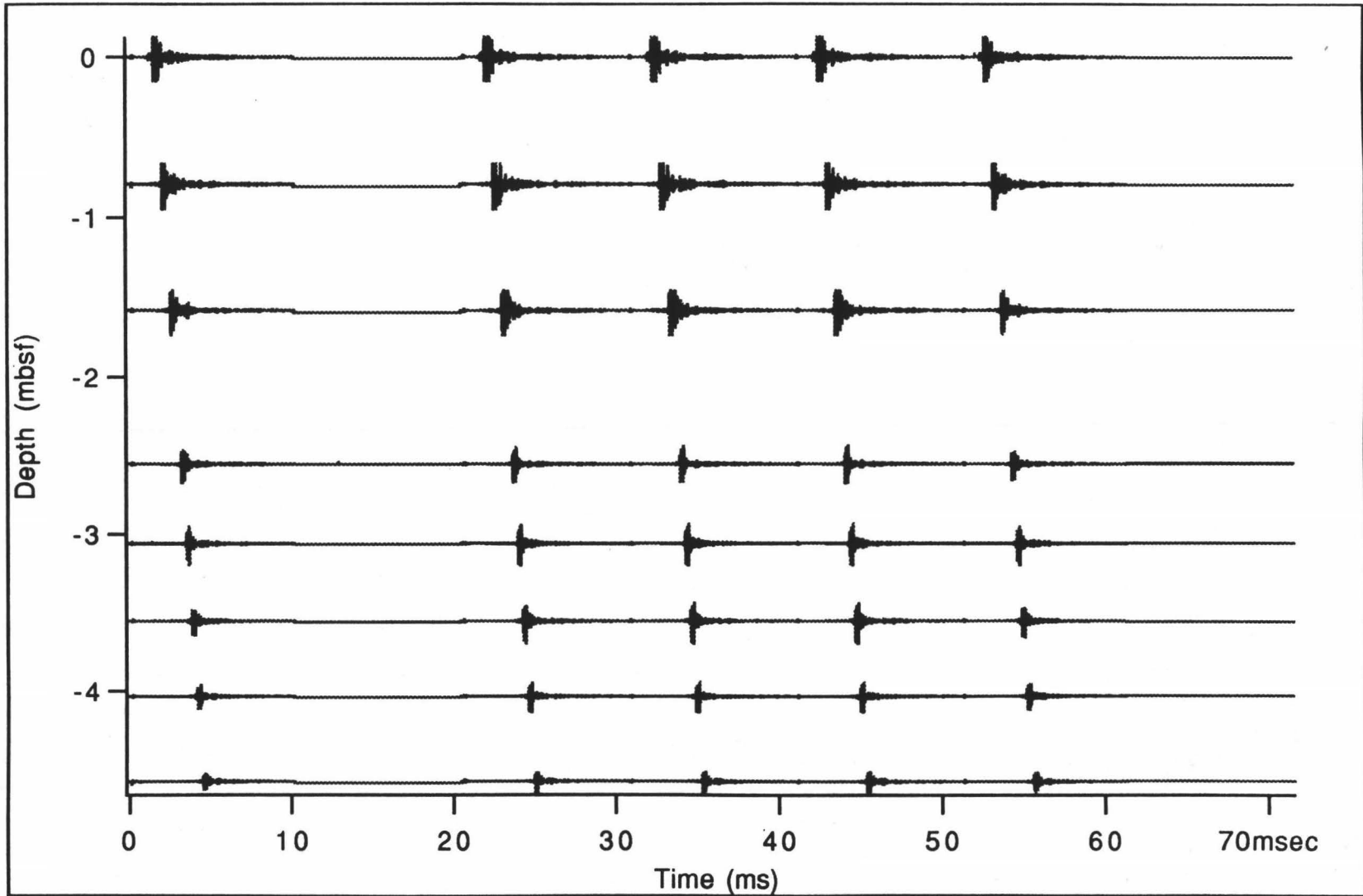


Figure 18. The waveforms of received signals from 5 stations (Station #1-Station #5) in a multiple-measurement deployment.

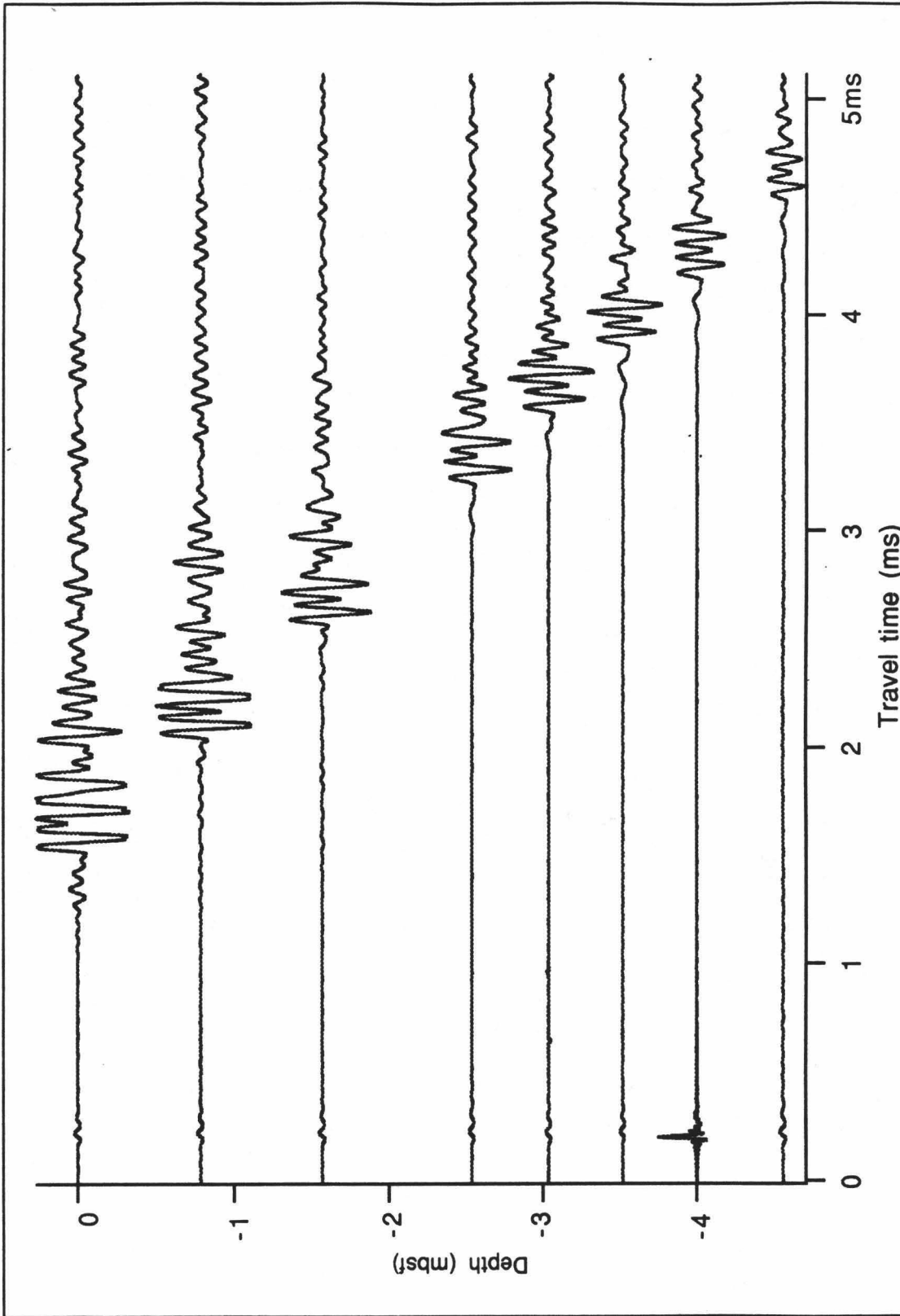


Figure 19. Waveform from one measurement at Station #6

Sample Measurements in the Laboratory

The P-wave velocity, wet-bulk density, grain density, porosity and calcite content of samples taken every 10 cm were measured in the laboratory. The P-wave velocity of the samples was determined by the travel time of sound waves in minicores about 2 x 2 x 2 cm³ in dimension. The frequency of measurement was about 300 kHz. The estimated error of the measurement is smaller than ± 10 m/sec, calibrated by measuring 3 standard pvc samples.

The wet-bulk density, grain density, porosity were determined by weight/volume relationship based on Hamilton's volume-of- sea-water method (Hamilton, 1971; Boyce, 1976).

Data Analyses and Results

The sedimentary layer of the upper several meters of seafloor contains the largest gradients in physical and acoustic properties in the sediment-water system. Few reports have provided profiles of in situ velocity and attenuation in this layer. Shirley and Anderson (1973, 1975) developed a compressional wave profilometer (pulse frequency 200 kHz) for continuously measuring sound speed and attenuation in sediments during a coring operation. They obtained some 12 m long in situ profiles of sound speed and attenuation in deep-water environments. Their results indicated that p-wave velocity does not usually increase with depth until depth exceeds twelve meters at their test sites . An in situ sediment acoustic measurement system (ISSAMS) of near surface geoacoustic properties (60 kHz p-wave velocity and attenuation, low frequency s-wave velocity) in shallow-water environments has been developed by Barbagelata et al. (1991). They presented representative data collected from the Adriatic Sea. Data showed that in situ and laboratory values of p-wave velocity were not significantly different at muddy sites, but at sandy sites laboratory measured values of p-wave velocity were 20-30 m/s higher than

in situ measured values of p-wave velocity in the uppermost 30 cm of seafloor. Badiey et al. (1988) conducted laboratory and in situ measurements of selected geoacoustic properties (shear modulus, frame loss coefficient, porosity, and permeability) in Great Bahama Bank shallow-water carbonate environments. The measured data showed that laboratory and in situ measurements of shear modulus and porosity are in good agreement, but permeability measurements in the laboratory were always somewhat lower than in situ values.

These results indicate that surficial sediment geoacoustic properties are complicated, and laboratory measurements of geoacoustic properties do not always agree with in situ measurements. Richardson et al. (1987) listed 11 factors that might contribute to the differences in laboratory and in situ measured values of some geoacoustic properties. In practice, however, it is difficult to figure out exactly which factors dominate in different environments.

In Situ Velocity Profiles

In situ velocity data with depth from 6 stations are listed in Table 2 and Table 3. Table 2 lists the 5 measurements at Station #6. It is obvious that the gravity corer did not penetrate into the sediment layers but fell down on the seafloor in the second and the third measurements at Station #6. The velocity remains constant with depth at a value of 1530 m/s (which is the velocity of the bottom water). The other 3 data set at Station #6 agree with each other, indicating proper penetration. Plots of in situ velocity versus depth of six stations are shown in Figure 20 (Station #6) and in Figure 21 (Station #1-Station #5). Data from Station #1- Station #6 consistently reveal a small acoustic low velocity channel just below the sediment-water interface of the sediment pond. We note that the Lance system can not indicate exactly its penetration depth when the core pipe does not penetrate completely into the sediment layer. In this situation the penetration depth is determined approximately by the velocities and recorded waveforms (look at the velocity

Table 2: The velocity data of 5 measurements in Station #6

The 1st measurement		The 2nd measurement		The 3rd measurement		The 4th measurement		The 5th measurement	
depth (mbsf)	velocity (m/s)	depth (mbsf)	velocity (m/s)	depth (mbsf)	velocity (m/s)	depth (mbsf)	velocity (m/s)	depth (mbsf)	velocity (m/s)
0	1530	0	1530	0	1530	0	1530	0	1530
0.784	1500	0.784	1530	0.784	1530	0.784	1500	0.784	1500
1.568	1500	1.568	1530	1.568	1530	1.752	1489	1.568	1500
2.536	1495	2.536	1530	2.536	1530	2.253	1507	2.536	1495
3.037	1518	3.037	1530	3.037	1530	2.735	1507	3.037	1518
3.519	1530	3.519	1530	3.519	1530	3.221	1543	3.519	1530
4.005	1543	4.005	1530	4.005	1530	3.772	1563	4.005	1543
4.556	1563	4.556	1530	4.556	1530			4.556	1563

Table 3: The velocity data of 5 stations (#1 - #5)

Station #1 measurement		Station #2 measurement		Station #3 measurement		Station #4 measurement		Station #5 measurement	
depth (mbsf)	velocity (m/s)	depth (mbsf)	velocity (m/s)	depth (mbsf)	velocity (m/s)	depth (mbsf)	velocity (m/s)	depth (mbsf)	velocity (m/s)
0	1530	0	1530	0	1530	0	1530	0	1530
0.784	1501	0.523	n *	0.261	n	0.261	n	0.784	1501
1.568	1500	1.307	1493	1.045	1493	1.045	1507	1.568	1493
2.536	1484	2.275	1484	2.013	1479	2.013	1497	2.536	1489
3.037	1507	2.776	1507	2.514	1507	2.514	1507	3.037	1507
3.519	1518	3.258	1506	2.996	1518	2.996	1506	3.519	1506
4.005	1531	3.777	1519	3.482	1495	3.482	1519	4.005	1543
4.556	1563	4.295	1541	4.033	1531	4.033	1541	4.556	1563

The velocity at 0 m (mbsf) is bottom water velocity.

*: n means no data.

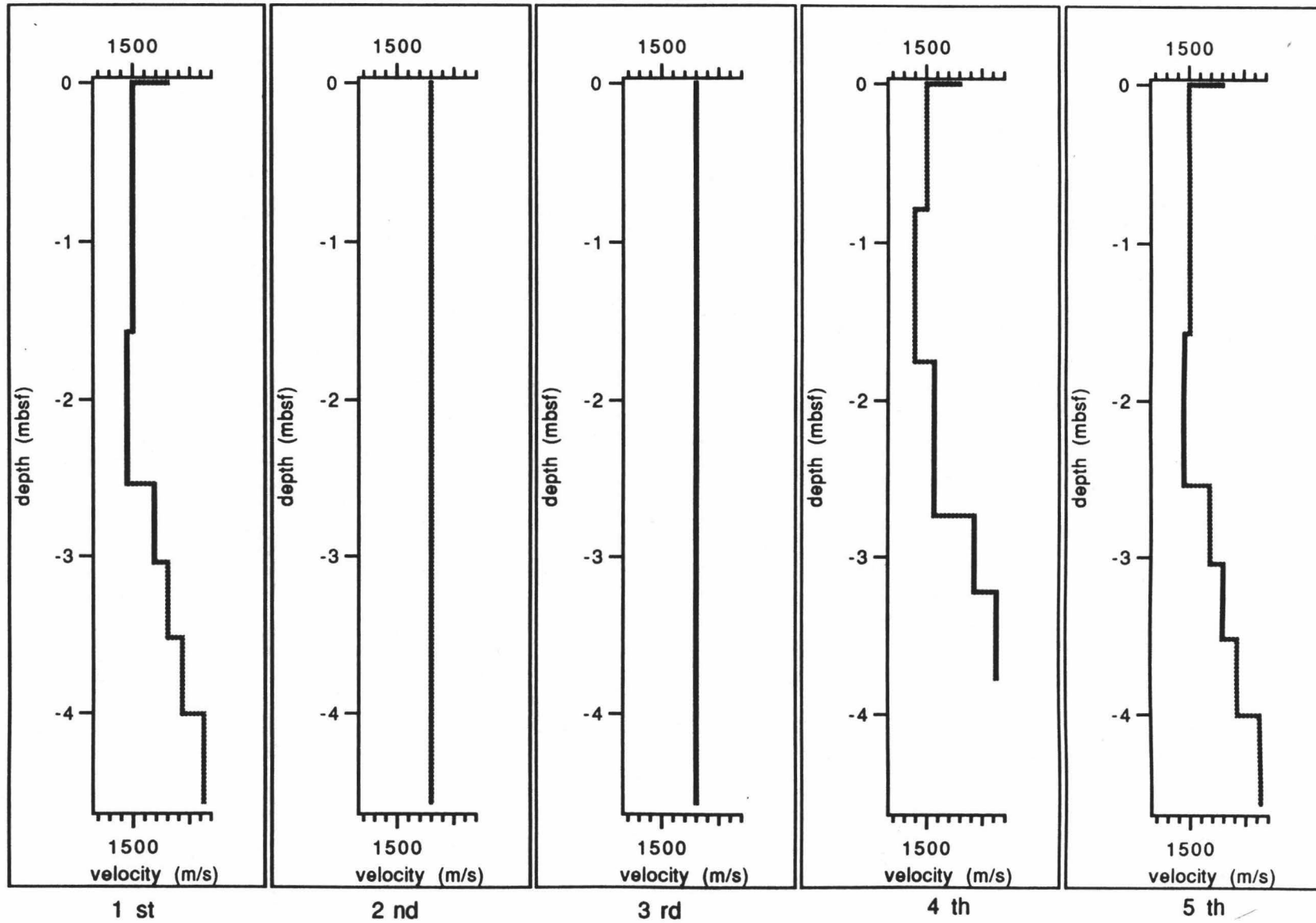


Figure 20. Velocity versus depth.
Measurements 1-5 at Station #6, in Site B' of the sediment pond

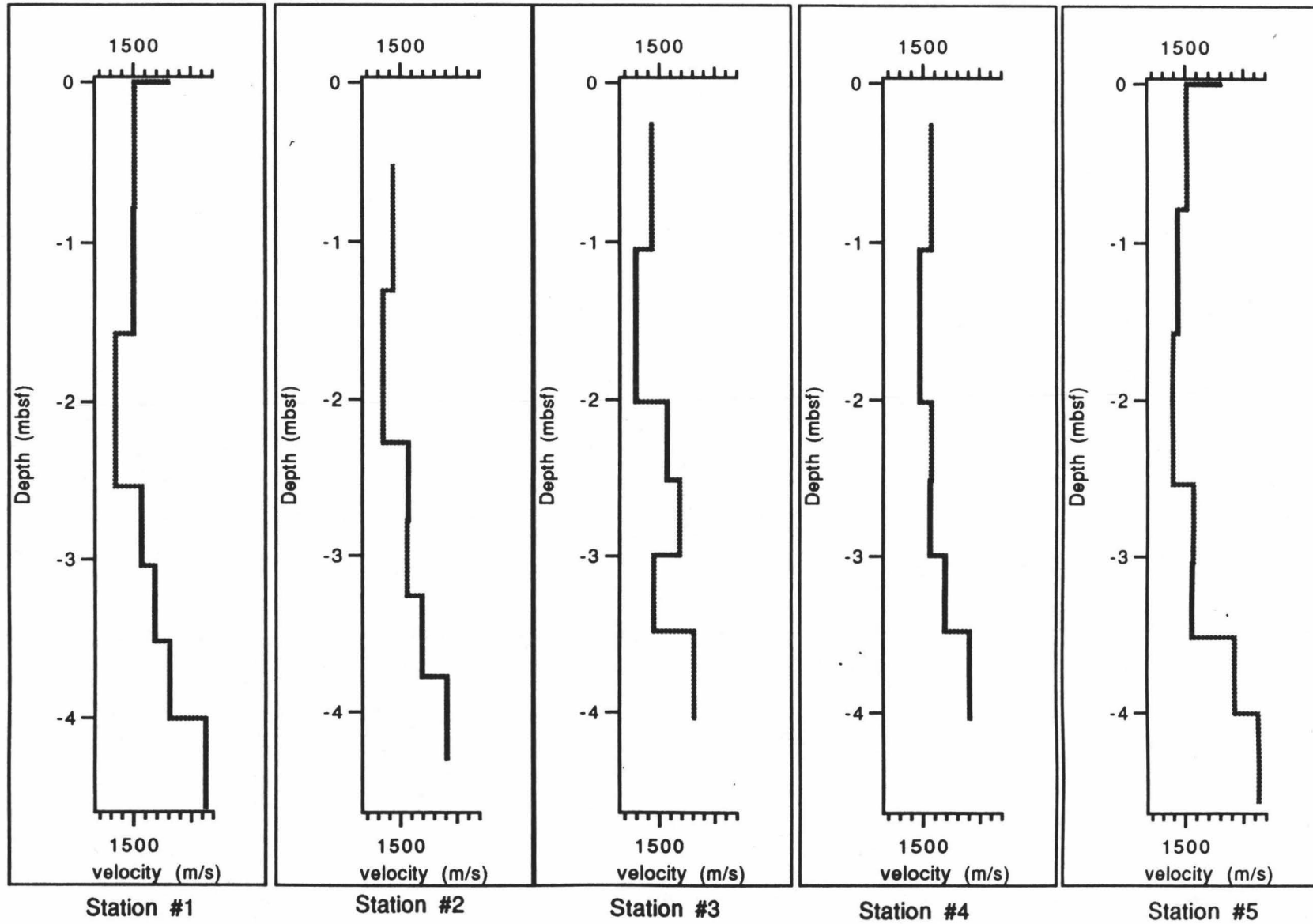


Figure 21. Velocity versus depth at 5 stations in Site A of the sediment pond

data of Station #2,#3, and #4 in Table 3; "n" means the top pair receivers are not completely in the sediment layer. The estimated error of penetration depth is about 1/3 receiver interval).

During studies of seismic-refraction measurements in the Atlantic Ocean, several investigators noted constant-frequency arrivals at long distance (Hersey et al., 1951; Officer, 1955; Katz and Ewing, 1956). These arrivals were interpreted as refraction along the ocean floor within a layer of low velocity. Katz and Ewing estimated depths of 20-45 m to the bottom of the acoustic channel at the Preliminary Mohole. Hamilton (1970) reviewed his and other investigators's results and concluded that the velocity ratio (sediment velocity/bottom water velocity) is usually less than 1, so a small acoustic channel is likely in the surface sediments. He concluded that such an acoustic channel should be present over large areas of the sea floor in most oceans of the world, including most deep-water areas and appreciable shallow-water areas. Hamilton defined the thickness of the acoustic channel (H_{ac}), by:

$$H_{ac} = (V_w - V_0) / a \quad (27)$$

where V_w is the velocity of the bottom water, V_0 is the surface sediment velocity, and a is the linear velocity gradient in the sediment. Hamilton suggested that most of these sediment acoustic channels in the deep-sea floor should be between 5 and 95 m thick with a linear velocity gradient 0.5 - 1.5 sec^{-1} .

Our results from the Atlantic sediment pond, however, indicate consistently that the velocity distribution in the upper several meters of seafloor sediments is quite complicated. In these layers, the velocity change may not be linear. The data of Station #1-Station #5 demonstrate that the velocity may decrease with depth in the uppermost 2 m of the layers, and then increase with depth after velocity arrives at a minimum value at 2 m mbsf. The velocity gradients in the uppermost 2 m of the sediment pond are about -25 sec^{-1} and turn to +25 sec^{-1} in the next lower 2 m of the layers. The data of Station #6

differ slightly from the results of Station #1-Station #5. The velocity data of Station #6 maintain a constant value of 1500 m/s in the top 2 m of sediments, and then increases with a gradient about $+25 \text{ sec}^{-1}$ within the lower 2.5 m of sediment.

After collecting more data Hamilton (1979) estimated the ranges of velocity gradient in marine sediments as $0.6 - 1.9 \text{ sec}^{-1}$. Ogushwitz (1985c) predicted with Biot's model that the velocity gradient varies in clays from $0.6 - 1.3 \text{ sec}^{-1}$. Our results refute their predictions for the upper several meters of clayey sea floor, such as a sediment pond. If we use formula (27) to define the acoustic channel thickness but the velocity change is more rapid than linear, the thickness of the acoustic channel may be only a few meters. The thickness of our measured acoustic channels is about 3.5-5 m.

Carlson et al. used Lance in the OBlique In-Situ Sonar Experiment project (OBIS) (1993) on a small delta in Kaneohe Bay of Oahu island, Hawaii. The test site consists of brown, volcanoclastic mud. They found that the water velocity is $1522 \pm 2 \text{ m}$ and that the velocity of the underlying sediment is $1475 \pm 30 \text{ m}$.

In conclusion, our data suggest that the acoustic channel is thinner than predicted by Hamilton (1979) and Ogushwitz (1985c), and that it is only a few meters in thickness lying just below the sea floor.

Laboratory Velocity Data

Because the deployments at Station #1-Station #5 were made by towing Lance, no core samples were recovered from these stations. A 2.2 m long core (Core #5) was recovered from a location very close to Station #6 thus permitting a comprehensive study of velocity distribution at the sediment-water interface. Velocity measured in the laboratory, measured in situ, and computed by Wood's equation (Wood, 1941) using porosity and density data measured in the laboratory (corrected to in situ conditions) are plotted in Figure 22. Figure 23 gives the procedure block diagram of the analysis of in situ data and laboratory data.

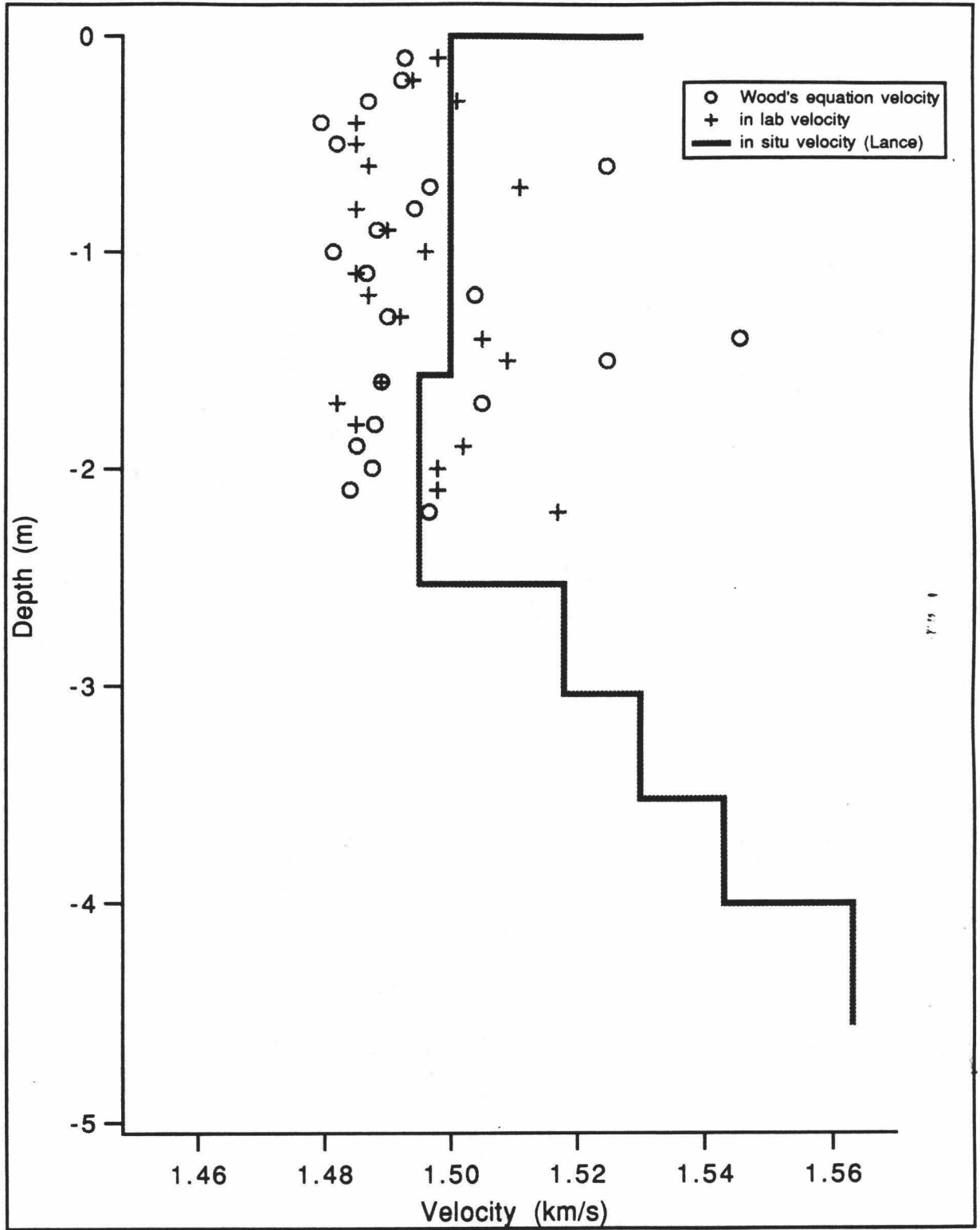


Figure 22. The comparison of velocity measurements at Station #6 in Site B' of the sediment pond.

The Analysis of In Situ Data and Laboratory Data

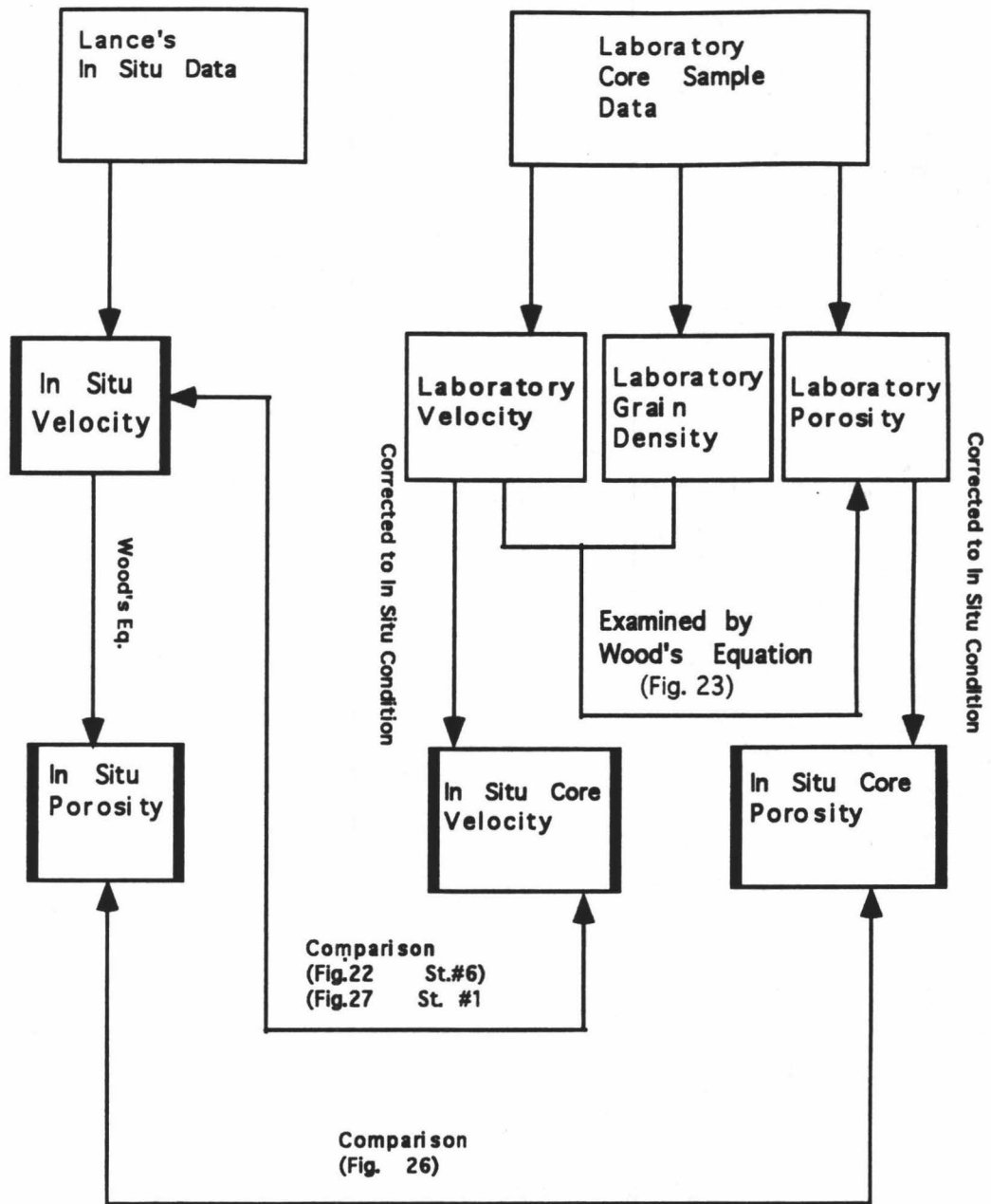


Figure 23. The procedure block diagram for analysis of in situ data and laboratory.

Wood's equation (Wood, 1941) describes a relationship between velocity and porosity of a high porosity aggregate of fluid and grains. Wood's theory assumes that the shear modulus of the aggregate of fluid and grains is zero, and that its bulk modulus is equal to a geometric average of bulk moduli of grains and fluid. According Wood's theory, the effective bulk modulus of the medium is given by:

$$1/K_{sed} = (\emptyset/K_w) + [(1+\emptyset)/K_g] , \quad (28)$$

where K_{sed} is bulk modulus of sediment, K_w is bulk modulus of seawater, \emptyset is porosity expressed as a fraction, and K_g is grain bulk modulus. Compressional velocity is then computed by:

$$V_p = \{ [K_{sed} + (4\mu/3)] / \rho \}^{1/2} \quad (29)$$

where ρ is bulk density of the seawater-sediment mixture and μ is the mixture shear modulus, here assumed to be zero. It can be seen that bulk modulus K_{sed} is strongly related to porosity \emptyset in Equation (28). Wood's equation has been shown to work well in describing the behavior of controlled laboratory clay mixtures of high porosity (Ogushwitz, 1985). Wilkens et al. (1992), based on their full waveform acoustic log data, suggested that Wood's estimation of the bulk modulus of the most porous sediments is fairly close to the dynamic bulk modulus.

The laboratory analyses of core recovered from Station #6 show a porosity range of 67%-81%. Wood's equation should work well in these porous sediments. In this case, the velocity measured in the laboratory is very close to the value corrected to in situ conditions because the pore water velocity at 23°C and 1 atmosphere pressure (1528 m/s) being is nearly the same as the in situ velocity of seawater (1530 m/s). According to Hamilton's velocity ratio method for correcting the laboratory velocity value to in situ (Hamilton, 1971), the correction is only 1 m/s. The three sets of measurements (Lance in

situ measurement, laboratory measurement and Wood's equation computation) seem to match well in the uppermost 2 m (Fig. 22). There are no core data available for comparison beneath 2 m.

Three cores (Core #1, Core #2 and Core #3) were recovered from locations across the sediment pond at Site A, adjacent to Station #1-Station #5. The ultrasonic velocity distributions of the three cores show different tendencies (Fig. 24). The ultrasonic velocity distribution of core #1 (2.8 m in length) shows the velocity increasing linearly with depth with a gradient of about $+15 \text{ sec}^{-1}$. Core #2 (1.8 m in length) and Core #3 (1.4 m in length) give a roughly constant ultrasonic velocity of 1520 m/s. It is expected that the sediments covering the sediment pond are homogeneous in a limited area. The Lance measurements (Fig.21) indicate that the five stations (Station #1 - Station #5) have quite similar in situ velocity distributions. The ultrasonic velocity distributions of the three cores, however, are not only inconsistent with the in situ measurements but also are inconsistent with each other.

We examined the relationship between ultrasonic velocity and porosity of the cores to determine whether our laboratory core measurements might have larger errors than we expected. The plot of ultrasonic velocity versus porosity of core samples is shown in Figure 25. The relationship between ultrasonic velocity and porosity of the cores agrees roughly with Wood's equation. The change of porosity with depth is different for each of the three cores (Fig. 24). The porosity of Core #1 roughly decreases with depth, but the porosity of Core #2 increases with depth from about 65% to 74%, and Core #3 shows a tendency toward constant porosity. Possibly these unconsolidated surface sediments are disturbed, or the surface part of the sediments has been lost during the coring and recovery processes.

Assuming that some soft surface sediments were lost during coring and recovery, a layered average porosity profile of Station #1 was calculated from the Lance in situ

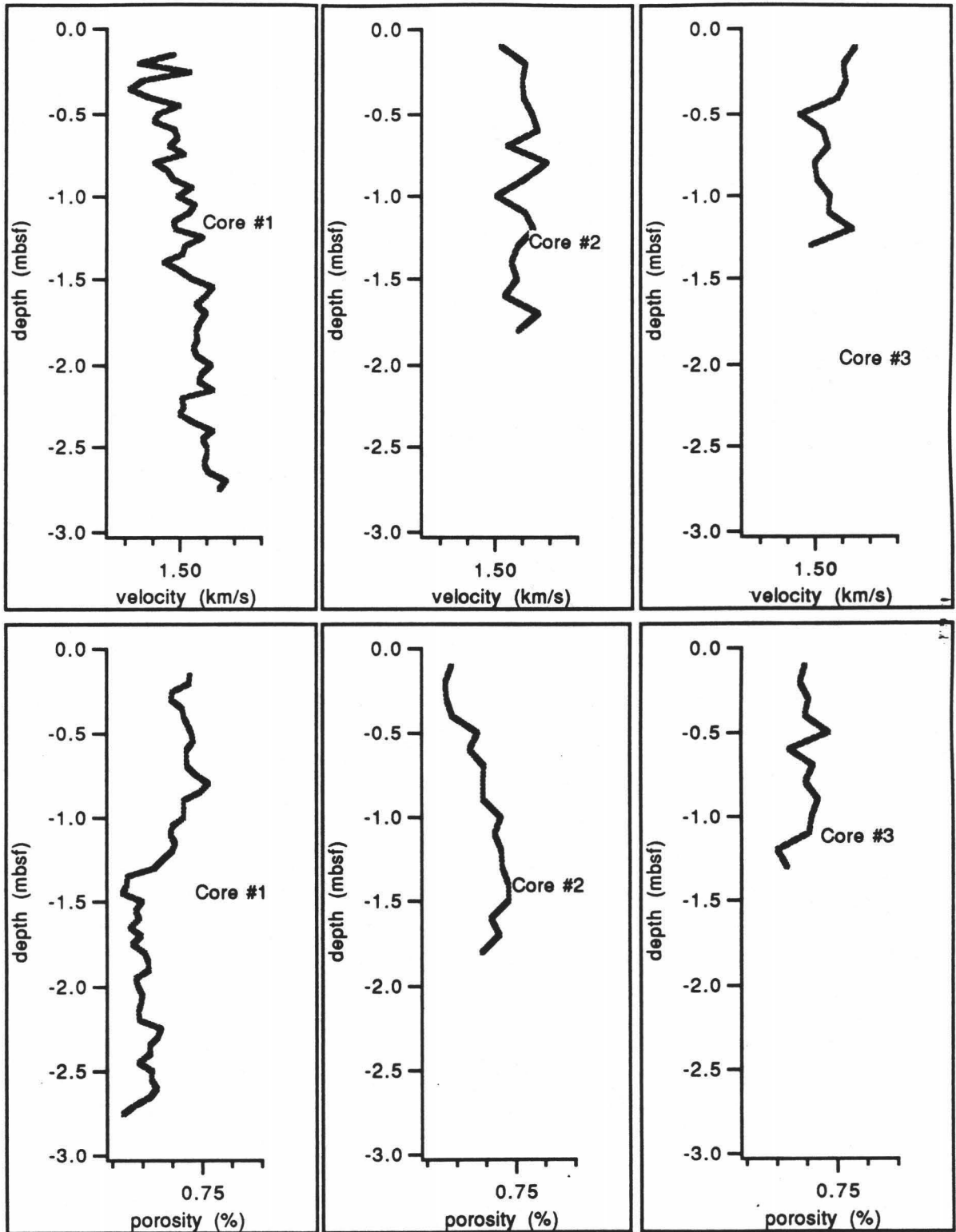


Figure 24. Velocity and porosity of Cores #1 - 3.

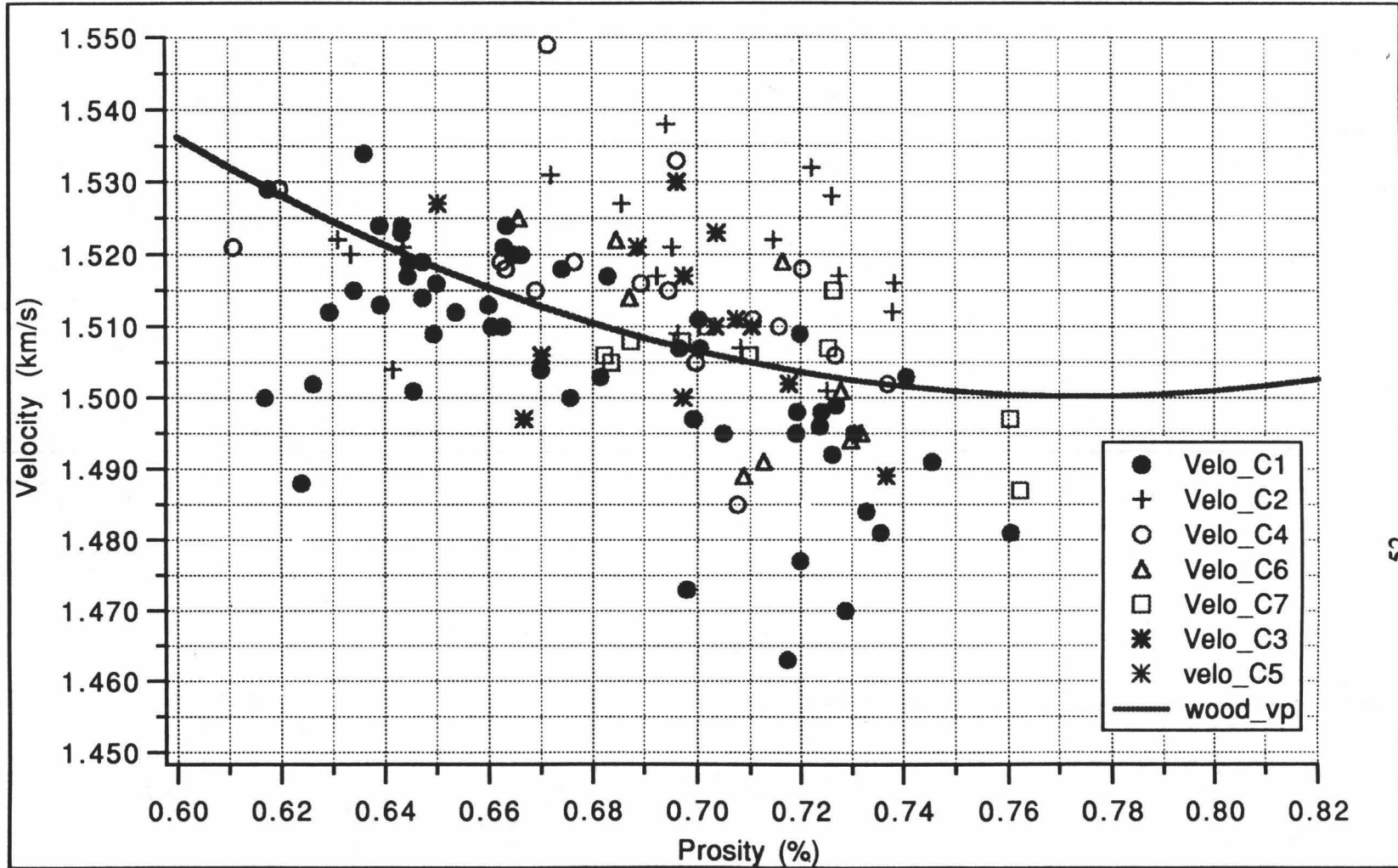


Figure 25. Velocity vs porosity measured in lab using 7 cores recovered from Site A and Site B of the sediment pond.

velocity data with Wood's equation (Fig. 26). As Figure 26 shows, if the porosity distributions with depth of Core #2 and Core #1 are offset down 0.8 meter, then one obtains a better fit to the calculated in situ porosity profile, especially for the Core #2 data. In the higher porosity range (about 60% - 100%), Wood's equation gives two values of porosity for a given velocity value. Wood's equation predicts that the velocity will have a minimum at porosity about 79% - 81% (a limit point of Wood's equation) under the in situ conditions of the sediment pond. Figure 27 shows two plausible porosity distributions calculated using Wood's equation. In Model A, the average porosity of the top 0.8 m of sea floor is about 93%. The velocity of the top layer is low, consistent with the porosity. Below the minimum, the velocity increases while porosity decreases. Model A is appropriate if Core #2 and Core #1 have lost 0.8 m of their uppermost sediments during the coring or recovering processes. In Model B, the average porosity of the top 0.8 m of sediment is 63% and the velocity monotonically increases with porosity decrease. As it is unlikely that core samples with about 63% - 73% porosity would be lost. We prefer Model A to Model B.

It should be noted that although Model A gives a better fit to the in situ porosity profile, the laboratory core velocity still does not match the in situ velocity data in Model A (Fig. 27). We question whether laboratory velocity data can be used to predict in situ seafloor velocity in sediment ponds.

A Hypothesis

The results of the Lance in situ measurements and the core measurements have been given above. It is interesting that the in situ data of six stations consistently show velocity begin to increase (with high gradient) at about 2 m depth below the seafloor, leading to the formation of a thin acoustic channel. This thin acoustic channel has not been seen in other reports. We propose a hypothesis (Fig. 28) to explain the phenomenon based on our in situ data. The surface sediments of about 2 m thickness, which cover the

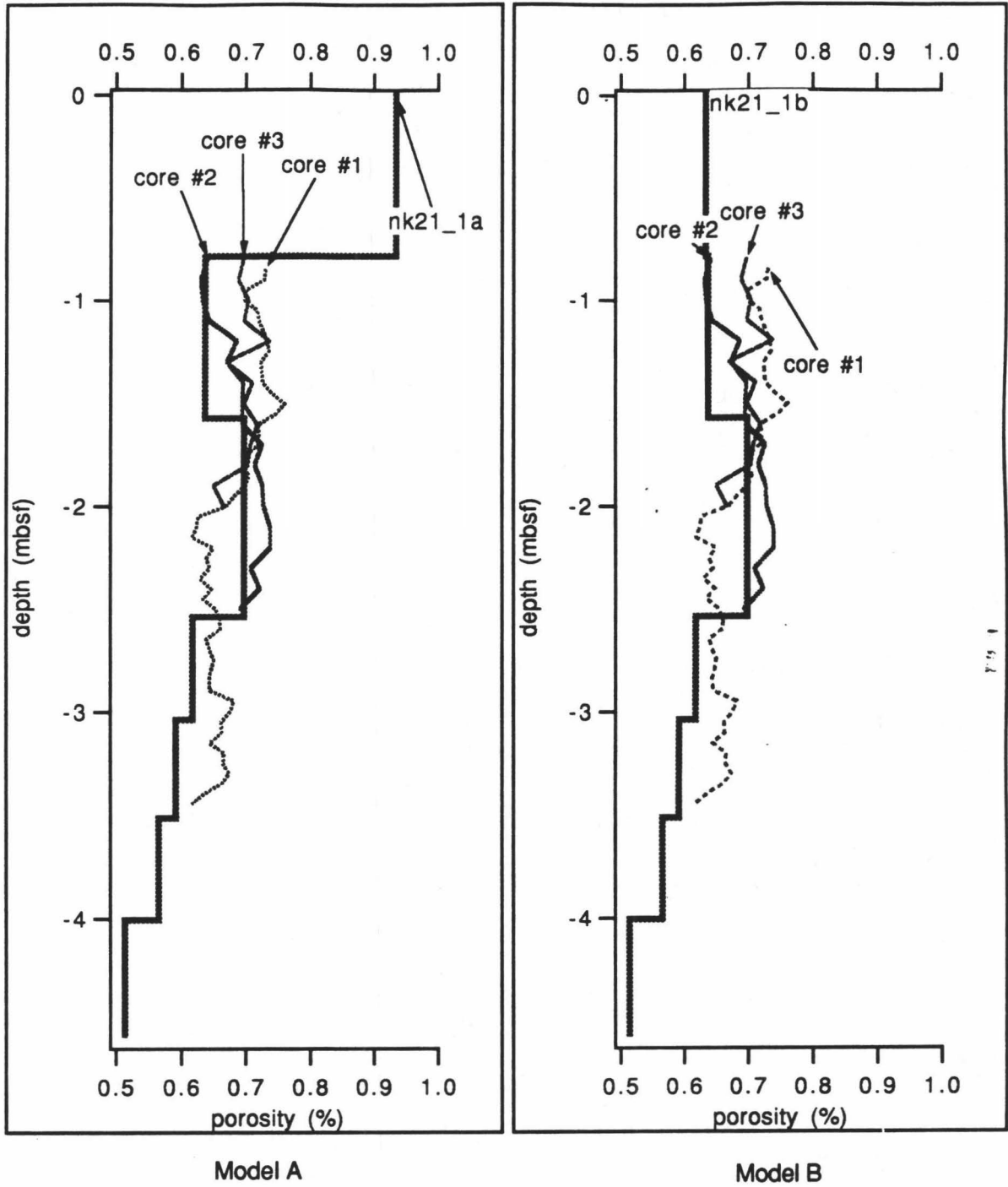


Figure 26. Two plausible models of porosity distribution.
 Core #1, core #2 and core #3 are porosity data measured in lab and offset down 0.8 m.
 Poro_A and poro_B are the porosities inverted from in situ velocity data using Wood's equation

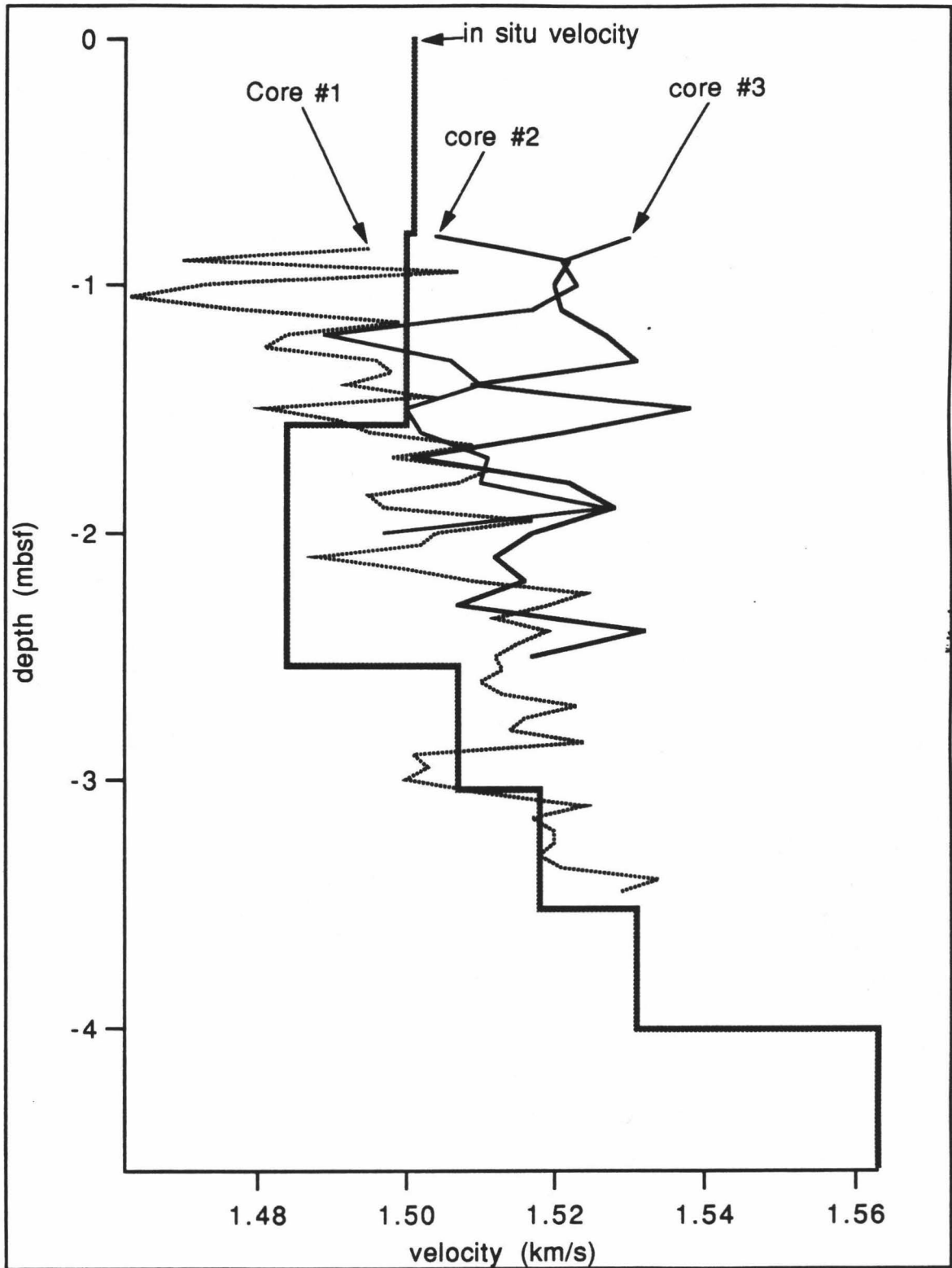


Figure 27. Velocity vs depth.
 Core #1, core #2 and core #3 are the velocities measured in lab and offset down 0.8 m.

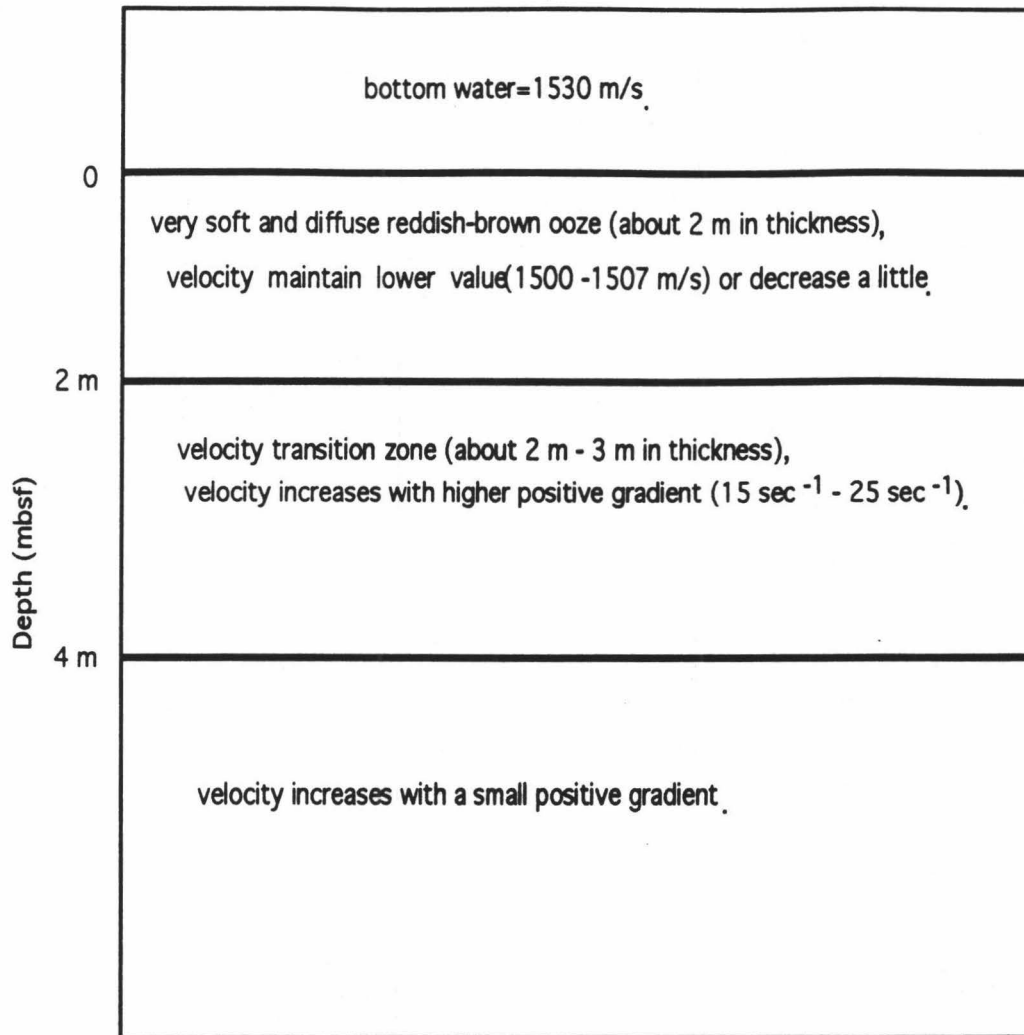


Figure 28. Sediment model inferred from data of this study

sediment pond, consist of very soft reddish-brown ooze. Below the layer, there would exist a transition zone a few meters where the process of consolidation occurs. Velocity increases with a high positive gradient within the transition zone due to the relative effects of consolidation. Above the transition zone, velocity would maintain a low value (same as that of surface sediment), or decrease a little because of the higher porosity of the sediments. Below the transition zone, the velocity increases with a small positive gradient where the relative effects of consolidation increase very slowly with depth.

In Situ Q Profile

As mentioned above, differences in receiver response functions produce large errors in the computation of Q. Unfortunately, no receiver response function data were obtained during the cruise that good enough for correcting Q. Accordingly, a rather simple procedure was used to roughly estimate a range for Q (Fig 29). Similar to selecting a proper truncation window in the spectral method, a signal received at the top receiver is used as a reference signal. A set of synthetic signals (Fig. 30) with different Q's are made according the formula:

$$S_s(\omega) = (L_1/L_2) S_0(\omega) \exp(i\omega x/c_0) \exp[-(\omega x)/(c_0 Q)] \quad (30)$$

where L_1 is the distance between the source transducer and the top receiver, and L_2 is the distance between the source transducer and the bottom receiver. (L_1/L_2) is the geometric spreading factor. The other symbols in the (30) are same as in equation (11). After comparing the synthetic signals with the signal received from the bottom receiver, we estimate the rough range of Q (Fig. 30) is greater than 60 and probably more than 80 at Station #1. Because the difference between the receiver response functions has been ignored in the model only a rough range of Q can be given.

Rough Q Estimation

(Receiver Response Function Has Been Ignored)

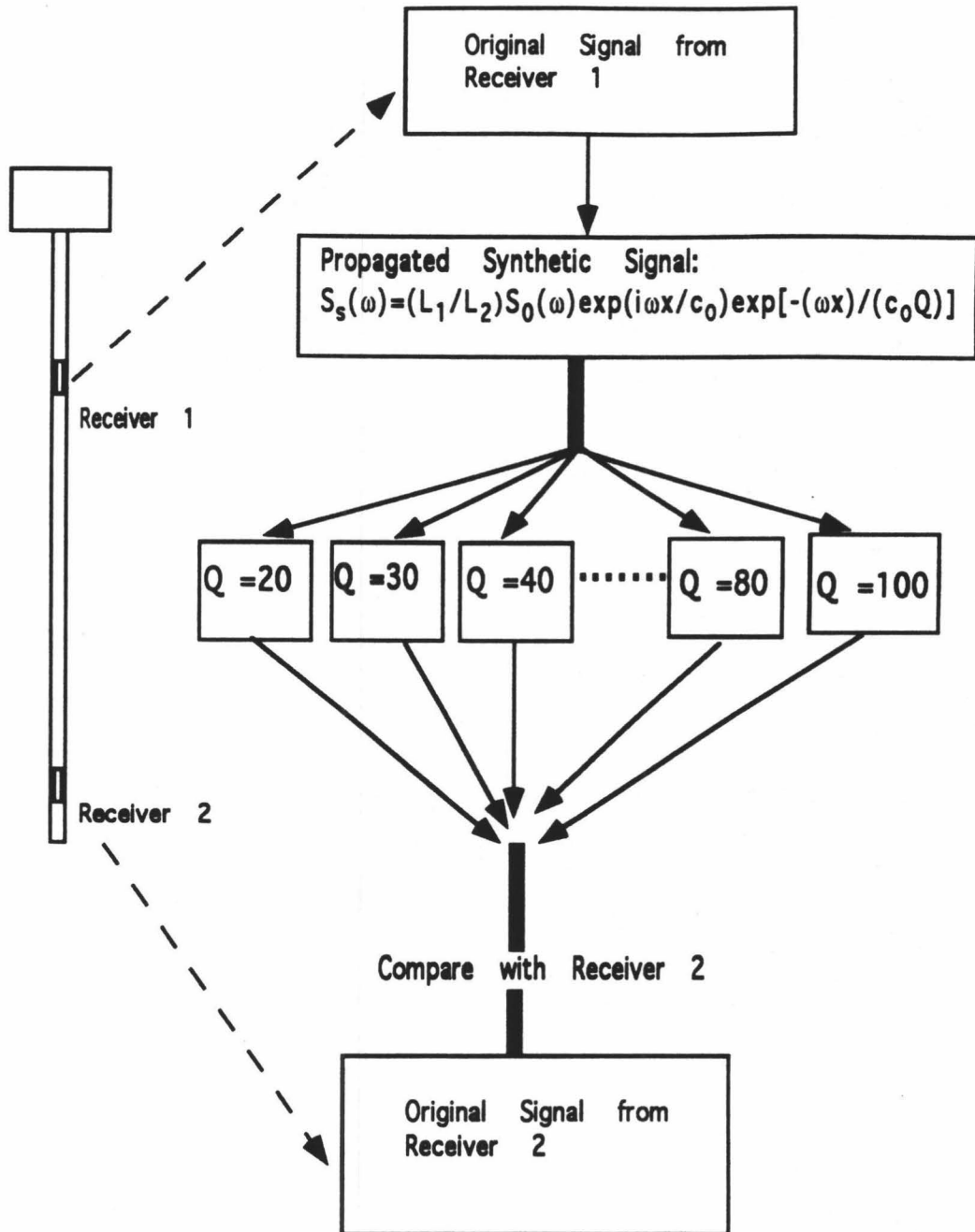


Figure 29. The procedure block diagram for rough Q estimation. Receiver response function has been ignored.

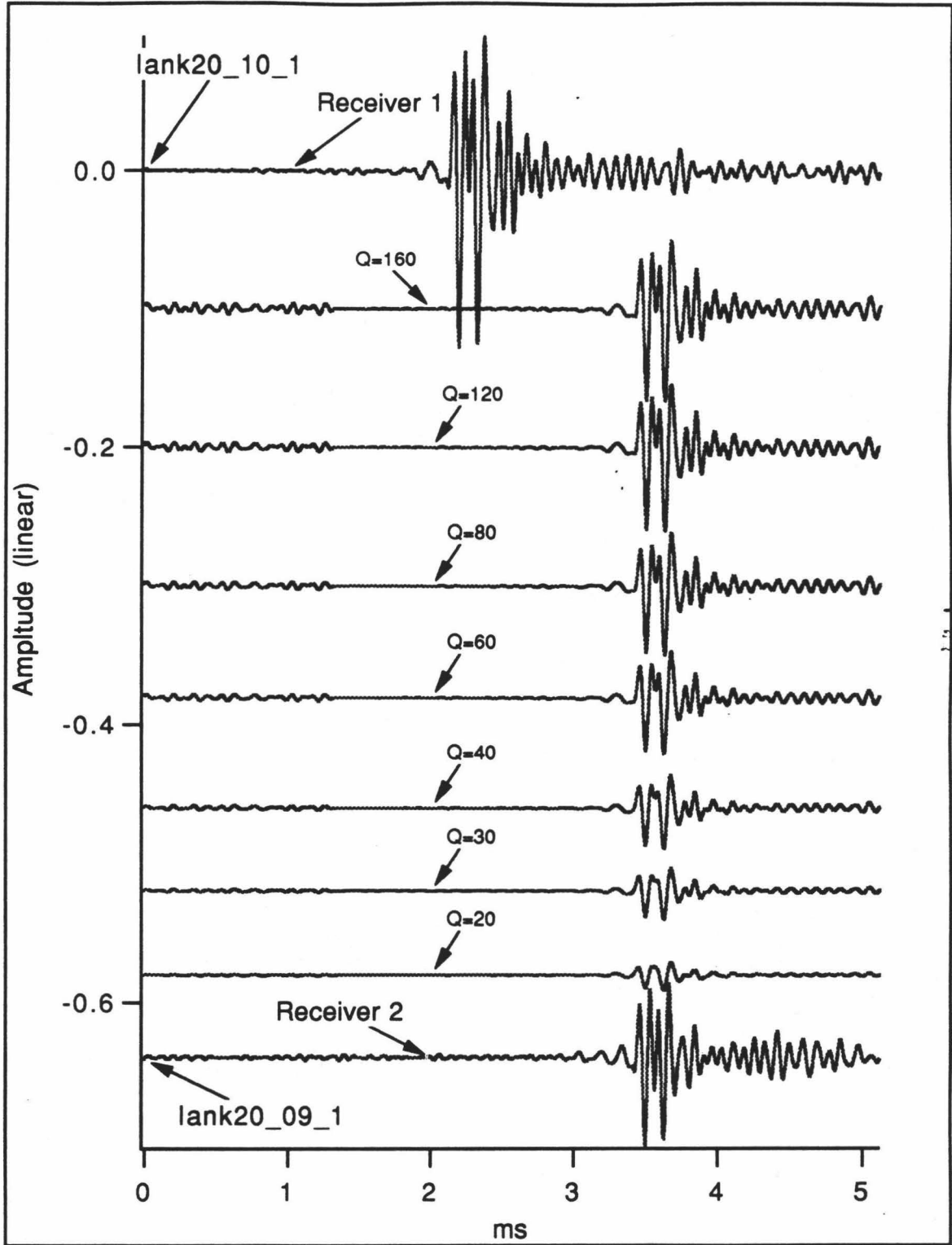


Figure 30. The estimation of Q by synthetic propagation.
 Signal from Receiver 1 is original reference signal.
 Synthetic propagation signals are compared with the signal from Receiver 2.

Discussion and Conclusions

Instrumentation

The Lance - the first instrument of its kind, a hybrid of heat-flow piston coring techniques with the principle of a full waveform acoustic logging tool, has proved a useful instrument for increasing our knowledge of the geo-acoustic structure of the sediment-seawater interface.

Most in situ velocity measurements of surficial sediments which have been reported are single points not profiles. Lance data give an actual in situ velocity profile and thus a velocity gradient. The velocity gradient is one of the dominant factors in the formation of an acoustic channel. Lance will be an important instrument in the study of acoustic channels in surficial marine sediments.

Velocity measurement of core samples has been used to predict the geo-acoustic structure of the seafloor for a long time. However, in surficial sediments such as very soft and diffuse clay or harder and unshaped sand, coring is very difficult. Therefore, the in situ measurements of Lance will be invaluable for these kinds of surficial sediments.

In Situ Experiment of the Sediment Pond

The results of the Lance experiments in the sediment pond along the flanks of the mid-Atlantic ridge have revealed some interesting things and left some unanswered questions.

1) The sedimentary layers of the upper several meters of seafloor may contain the largest gradients in physical and acoustic properties in the sediment-water system. Both the in situ data and the core data of the sediment pond have indicated the complexity of this zone.

- 2) The data from 6 stations of the sediment pond consistently show a thin (few meters in thickness) acoustic channel which differs from the prediction in clayey seafloor of Hamilton (1979) and Ogushwitz (1985).
- 3) The core data from Station #6, in Site B' of the sediment pond agree well with the in situ data of Lance. The data from three cores recovered from the adjacent locations of Station #1-Station #5, in Site A of the sediment pond not only disagree with the in situ data of Station #1-Station #5, but also do not agree well with each other, while the in situ velocity data display a consistent velocity distribution. Possibly the soft surface sediments were disturbed or lost during the coring and recovering processes.
- 4) Although our results are preliminary and subject to verification by further experiment, they suggest strongly that core data can not reliably be used to predict in situ acoustic properties of surface sediment in areas where these sediments are very soft. In such areas in situ acoustic properties can only be determined by direct in situ measurement, using devices such as Lance.

References

- Biot, M. A., 1956. Theory of propagation of elastic waves in a fluid-saturated porous solid. I. Low frequency range. *J. Acoust. Soc. Am.*, 28, 168 -178.
- Biot, M. A., 1956. Theory of propagation of elastic waves in a fluid-saturated porous solid. II. Higher frequency range. *J. Acoust. Soc. Am.*, 28, 179-191.
- Biot, M. A., 1962. Mechanics of deformation and acoustic propagation in porous media. *J. Appl. Phys.*, 33: 1482 -1498.
- Badiey, M., Tamamoto T., Turgut, A., Bennett, R. & Conner, C. S., 1988. Laboratory and in situ measurements of selected geoacoustic properties of carbonate sediments. *J. Acoust. Soc. Am.*, 84, 689-696.
- Barbagelata, A., Richardson, M., Miaschi, B., Muzi, E., Guerrini, P., Troiano, L. & Akal, T., 1991. ISSAMS: An in situ sediment acoustic measurement system. Shear Wave In Marine Sediment, edit by Hovem, J. M., Richardson, M. D. & Stoll, R. D. Kluwer Academic Publishers, Netherlands. pp. 305-312.
- Boyce, R. E., 1976. Definitions and laboratory techniques of compressional sound velocity parameters and wet-water content, wet-bulk density, and porosity parameters by gravimetric and gamma ray attenuation techniques. Library of Congress Catalog Card Number 74-603338, Washington, D. C. 1976.
- Bromirski, P. D., Frazer, L. N. & Duennebier, F. K., 1992a. Sediment shear Q from airgun OBS data. *Geophys. J. Int.* 110: 465 - 485.
- Bromirski, P. D., Frazer, L. N. & Duennebier, F. K., 1992b. Sediment shear Q from pulse width measurements. Estimating the pulse width constant. *EOS, Trans., Am. Geophys. Un.*, 73: 593, abs.
- Bromirski, P. D., Frazer, L. N. & Duennebier, F. K., 1994. The Q-gram method: Q from instantaneous phase. *Geophys. J. Int.* (in press.)

- Carlson, R. L., Gangi, A. F. & Wilkens, R. H., 1994. Oblique in-situ sonar experiment - OBS. A proposal to ONR.
- Hamilton, E. L., 1970. Sound channels in surficial marine sediments. *J. Acoust. Soc. Am.*, 48: 1296 -1298.
- Hamilton, E. L., 1971. Prediction of in situ acoustic and elastic properties of marine sediments, *Geophysics* 36, 266 -284.
- Hamilton, E. L., 1974. Geoacoustic models of sea floor. Physics of Sound in Marine Sediments, edit by L. Hampton. Plenum, New York, 1974. pp. 181 -221.
- Hamilton, E. L., 1976. Sound attenuation as a Function of depth in the sea floor. *J. Acoust. Soc. Am.*, 59 : 528 - 535.
- Hamilton, E. L., 1979. Sound velocity gradient in marine sediments. *J. Acoust. Soc. Am.*, 65: 909 - 992.
- Hamilton, E. L., 1980. Geoacoustic modeling of sea floor. *J. Acoust. Soc. Am.*, 68 : 1313 -1340.
- Hamilton, E. L., 1987. Acoustic properties of sediments. Acoustics and Ocean Bottom, edited by A. Lara -sanz, C. Ranz Guerra, and C. Carbofite. Madrid 1987.
- Hersey, J. B., Officer, C. B., Johnson, H. R., & Bergstrom, S., 1951. Seismic refraction observation north to the Brownson. *Bull. c Seismol. Soc. Amer.*, 42: 291 - 306.
- Jacobson, R. S., 1987. An investigation into the fundamental relationships between attenuation, phase dispersion, and frequency using seismic refraction profiles over sedimentary structure. *Geophysics*, 52: 72 - 87.
- Jannsen, D., Voss, J. & Theilen, F., 1985. Comparison of methods to determine Q in shallow marine sediments from vertical reflection seismograms. *Geophys. Prosp.*, 33: 479 - 497.

- Johnston, D. H. & Toksoz, M. N., 1981. Seismic wave attenuation--definition and terminology, in Seismic Wave Attenuation, pp. 1-5, edit by Toksoz, M. N. & Johnston, D. H., SEG Geophysics reprint series No. 2, Tulsa.
- Kanamori, H. & Anderson, D. L., 1977. Importance of physical dispersion in surface wave and free oscillation problems: Review. *Rev. Geophys. Space Phys.*, 15: 105 -112.
- Katz, S. & Ewing, M., 1956. Seismic-refraction measurement in the Atlantic Ocean Part VII: Atlantic Ocean Basin, West of Bermuda. *Geol. Soc. Amer. Bull.* 67: 475 - 510.
- Kibblewhite, A. C., 1989. Attenuation of sound in marine sediments: A review with emphasis on new low -frequency data. *J. Acoust. Soc. Am.*, 86 (2): 716 - 738.
- Kjartansson, E., 1979. Constant Q-wave propagation and attenuation., *J. Geophys. Res.*, 84: 4737 - 4748.
- McCann, C. and McCann, D. M., 1969. The attenuation of compressional waves in marine sediments. *Geophysics.* 34, 882 - 892.
- O'Connell, R.J. & Budiansky, B., 1978. Measures of dissipation in viscoelastic media. *Geophys. Res. Lett.*, 5: 5 - 8.
- Officer, C. B., 1955. Deep sea seismic reflection profile. *Geophysics.* 20: 270 -282.
- Ogushwitz, P. R., 1985a. Applicability of Biot theory. I. Low - porosity materials. *J. Acoust. Soc. Am.*, 77 (2): 429 - 440.
- Ogushwitz, P. R., 1985b. Applicability of Biot theory II. Suspensions. *J. Acoust. Soc. Am.*, 77 (2): 441 - 452.
- Ogushwitz, P. R., 1985c. Applicability of Biot theory. III. Wave speeds versus depth in marine sediments. *J. Acoust. Soc. Am.*, 77 (2): 453 - 464.
- Richardson, M. D., Curzi, P. V., Muzi, E., Miaschi, B., and Barbagelata, A., 1987. Measurement of shear wave velocity in marine sediments. In: Acoustics and Ocean

- Bottom II FASE Specialized Conference. edit by LaraSaenz, A., Ranz-Guerra, C. and Carbo, C. , Consejo Superior de Investigaciones Cientificas, Madrid, P. 75-84.
- Plona, T. J., 1980. Observation of second bulk compressional wave in a porous medium at ultrasonic frequencies. *App. Phys. Lett.* 36: 259 - 261.
- Shirley, D. J., Anderson, A. L. & Hampton, L. D., 1973a. In situ measurements of sediment sound speed during coring. Applied Research Laboratories Technical Report No. 73-1 (ARL-TR-73_1), Applied Research Laboratories, The university of Texas at Austin, Austin, Texas.
- Shirley, D. J., Anderson, A. L. & Hampton, L. D., 1973b. Measurement of in situ sound speed during sediment coring. OCEAN ' 73, Proceedings of the IEEE International Conference on Engineering in the Ocean Environment, Seattle, Washington.
- Shirley, D. J. & Anseron, A. L., 1975. In situ measurement of marine sediment acoustical properties during coring in deep water. *IEEE Transactions on Geoscience Electronics*, GE-13, NO. 4.
- Spencer, J. W., 1981. Stress relaxations at low frequencies in fluid saturated rock: attenuation and modulus dispersion. *J. Geophys. Res.* 86, 1803 -1812.
- Stansfield, D. 1990. Underwater Electroacoustic Transducers. Bath University Press and Institute of Acoustics.
- Stoll, R. D., 1985. Marine Sediment acoustics. *J. Acoust. Soc. Am.*, 77: 1789 -1799.
- Wilkens, R. H., Cheng, C. H. & Meredith, J. A. 1992. Evaluation and prediction of Shear wave velocity in calcareous marine sediment and rock. *J. Geophys. Re.* 97: 9297 - 9305.
- Wood. A. B., 1941. A Textbook of Sound. G. Bell and Sons, Ltd, London.